Aus dem Zentrum für Innere Medizin der Universität zu Köln
Klinik und Poliklinik für Innere Medizin I
Direktor: Universitätsprofessor Dr. med. M. Hallek

Elucidating the effect of anti-VEGF-A and anti-ANG-2 in combination with immunecheckpoint inhibition targeted treatment in small cell lung cancer

Inaugural-Dissertation zur Erlangung der Doktorwürde
der Medizinischen Fakultät der Universität zu Köln

vorgelegt von
Christoph Julius Otto
aus Nürnberg

promoviert am 31. Oktober 2023

Gedruckt mit Genehmigung der Medizinischen Fakultät der Universität zu Köln
2023

Dekan: Universitätsprofessor Dr. med. G. R. Fink
1. Gutachter: Universitätsprofessor Dr. med. Dr. nat. med. R. T. Ullrich
2. Gutachterin: Universitätsprofessorin PhD C. M. Niessen

Erklärung

Ich erkläre hiermit, dass ich die vorliegende Dissertationsschrift ohne unzulässige Hilfe Dritter und ohne Benutzung anderer als der angegebenen Hilfsmittel angefertigt habe; die aus fremden Quellen direkt oder indirekt übernommenen Gedanken sind als solche kenntlich gemacht.

Bei der Auswahl und Auswertung des Materials sowie bei der Herstellung des Manuskriptes habe ich Unterstützungsleistungen von folgenden Personen erhalten:
Frau PD Dr. Lydia Meder

Weitere Personen waren an der Erstellung der vorliegenden Arbeit nicht beteiligt. Insbesondere habe ich nicht die Hilfe einer Promotionsberaterin/eines Promotionsberaters in Anspruch genommen. Dritte haben von mir weder unmittelbar noch mittelbar geldwerte Leistungen für Arbeiten erhalten, die im Zusammenhang mit dem Inhalt der vorgelegten Dissertationsschrift stehen.

Die Dissertationsschrift wurde von mir bisher weder im Inland noch im Ausland in gleicher oder ähnlicher Form einer anderen Prüfungsbehörde vorgelegt.

Die dieser Arbeit zu Grunde liegenden Ideen und Konzepte sind größtenteils unter Anleitung von Univ.-Prof. Dr. Dr. R. Ullrich und PD Dr. Lydia Meder entstanden. Die in dieser Arbeit angegebenen Experimente sind nach entsprechender Anleitung durch Frau PD Dr. Lydia Meder größtenteils von mir selbst ausgeführt worden. Die Auswertung der hierbei entstandenen Daten führte ich nach entsprechender Anleitung durch Frau Meder eigenständig durch. Dabei standen die folgenden Software-Programme Excel®, Kaluza®, GraphPad Prism® bei der Analyse und Darstellung im Vordergrund. Bei der bioinformatischen Auswertung der RNA-Sequenzierung wurde ich von Herrn Dr. med. Sven Borchmann angeleitet und unterstützt. Bei der Durchführung der Proteinanalyse mittels WesternBlot wurde ich von Frau Mirjam Koker, BSc angeleitet und unterstützt. Die Behandlungen und Messungen an den Versuchstieren wurden gemeinsam mit Frau PD Dr. Lydia Meder und der medizinisch-technischen Assistentin Frau Marieke Nill durchgeführt.

Diese Arbeit ist teilweise in Anlehnung und Zusammenarbeit mit der noch unveröffentlichten Publikation mit dem vorläufigen Titel „*Blocking the Angiopoietin-2/integrin beta-1 signaling axis abrogates tumor cell invasion and metastasis in small cell lung cancer*" von Meder *et al.* (Ersteinreichung am 18.10.2022 bei „*JCI Insight",* Manuskript 166402-INS-RG-1) entstanden. Weitere in der Publikation gelistete Mitautoren waren an der Entstehung dieser Arbeit über diesen Weg mittelbar beteiligt. In dieser Arbeit werden Inhalte, die aus der noch unveröffentlichten Publikation Meder *et al.* mit freundlicher Genehmigung übernommen wurden, entsprechend zitiert und als *„under revision"* gekennzeichnet. Das schriftliche Einverständnis von Univ.-Prof. Dr. Dr. Roland Ullrich über die Vorabveröffentlichung von Teilergebnissen in dieser Arbeit liegt vor.

Erklärung zur guten wissenschaftlichen Praxis:

Ich erkläre hiermit, dass ich die Ordnung zur Sicherung guter wissenschaftlicher Praxis und zum Umgang mit wissenschaftlichem Fehlverhalten (Amtliche Mitteilung der Universität zu Köln AM 132/2020) der Universität zu Köln gelesen habe und verpflichte mich hiermit, die dort genannten Vorgaben bei allen wissenschaftlichen Tätigkeiten zu beachten und umzusetzen.

Köln, den 28.01.2023

Christoph Otto

TABLE OF CONTENT:

ABBREVIATIONS

ALK	Anaplastic lymphoma kinase
ANG2	Angiopoietin-2
ANGPT2	Angiopoietin-2
APC	Antigen presenting cell
ASCL1	Achaete-scute homolog 1
B2M	Beta 2 microglobulin
BW	Bodyweight
CD	Cluster of differentiation
CDK6	Cyclin dependent kinase 6
CNS	Central nervous system
CR	Complete response
CTL	Cytotoxic T-lymphocytes
CTLA4	cytotoxic T-lymphocyte-associated Protein 4
DLL3	Delta like protein 3
DPBS	Dulbecco's Balanced Salt Solution
EC	Endothelial cell
ECM	Extracellular matrix
ECOG	Eastern Cooperative Oncology Group
EGF-R	Epidermal-Growth-Factor-Receptor
EML4-ALK	echinoderm microtubule-associated protein-like 4 and Anaplastic lymphoma kinase fusion gene
EMT	Epithelial to mesenchymal transition
ES	Extensive Stage
FACS	Fluorescence Activated Cell Sorting
FAK	Focal adhesion kinase
FFPE	formalin-fixed paraffin-embedded
ICAM1	Intercellular cell adhesion molecule 1
ICB	Immune checkpoint blockade
IFN-g	Interferon gamma
IgG	Immunoglobulin G
IHC	Immunohistochemistry
IL	Interleukin
LS	Limited Stage
M-CSF	Macrophage colony stimulating factor

MAPK	Mitogen-activated protein kinase
MDSC	Myeloid-derived suppressor cell
MHC	major histocompatibility complex
MIP-1a	Macrophage inflammatory protein 1a
MIP-2	Macrophage inflammatory protein 2
mRNA	Messenger ribonucleic acid
NCAM	Neural cell adhesion molecule
NE	Neuroendocrine
NSCLC	Non-small cell lunger cancer
OS	Overall survival
p	Phosphorylated
PCI	Prophylactic cranial irradiation
PD	Progressive disease
PD-1	programmed cell death protein 1
PD-L1	programmed cell death 1 ligand
PFS	Progression free survival
PI3K	Phosphoinositid-3 kinase
PMSF	Phenylmethylsulfonylfluorid
PR	Partial response
PTEN	Phosphatase and Tensin homolog
Rb1	Retinoblastoma 1
RECIST	Response Evaluation Criteria in Solid Tumors
RNA	Ribonucleic acid
SCLC	Small cell lung cancer
SD	Stable disease
SEM	Standard error of the mean
SH2	Src-homology 2
STAT3	Signal transducer and activator of transcription 3
TAM	Tumor associated macrophage
TBST	Tris-buffered saline with Tween20
TCR	T-cell receptor
TEMs	TIE2-expressing monocytes
TIE2	ANG-2 receptor
TIM-3	mucin-domain containing-3
TKI	Tyrosine kinase inhibitor

TMB	Tumor mutational burden
TME	Tumor micro-environment
TNM	TNM -classification: Tumor, Nodes, Metastases
T_{reg}	Regulatory T-cells
VCAM-1	Vascular cell adhesion molecule 1
VEGF-A	Vascular endothelial growth factor A
VEGF-A-KO	VEGF-A knockout
VEGFR	VEGF receptor
VEGFRi	VEGF receptor inhibitor
Y	Amino acid tyrosine
µCT	Micro computed tomography

1 ZUSAMMENFASSUNG

Unter den verschiedenen Lungenkrebs-Subtypen macht das kleinzellige Lungenkarzinom (engl. small cell lung cancer, SCLC) etwa 15% der Diagnosen aus. Diese Unterart zeichnet sich durch ein außerordentlich schnelles Fortschreiten der Erkrankung sowie durch eine besonders schlechte Prognose aus. Die Behandlung des SCLC erfolgt mit Platin-basierter Chemotherapie und kann seit 2018 durch Immuntherapie in Form von Atezolizumab, einem PD-L1 blockierenden Antikörper, ergänzt werden. Eine häufige Hürde in der Therapie des SCLC ist dessen Eigenschaft, dem gegen den Tumor gerichteten Immunsystem gezielt entgehen zu können. Das allgemeine Ziel der Immuntherapie ist die Wiederherstellung der gegen den Tumor gerichteten Immunantwort, sodass das Immunsystem den Tumor wieder wirksam bekämpfen kann. Insbesondere bei der Behandlung des SCLC können solche immuntherapeutischen Effekte jedoch unter anderem durch eine unzureichende Infiltration des Tumors mit Immunzellen limitiert werden. Dieser Zustand wird wiederum durch die dysfunktionale Gefäßarchitektur des Tumors begründet, der hohe Spiegel der pro-angiogenen Faktoren vaskulärer endothelialer Wachstumsfaktor A (VEGF-A) und Angiopoietin-2 (ANG-2) zugrunde liegen. Um den tumor-fördernden Effekten entgegenzuwirken, haben wir in unserer Studie die Immuntherapie um anti-angiogene Therapie erweitert.

In meiner Dissertation konnte ich zeigen, dass durch die Kombination von PD-1, ANG-2 und VEGFR Blockade das Überleben von SCLC tragenden Mäusen signifikant gesteigert wurde. Dabei konnte die Blockade von ANG-2 und VEGFR die anti-PD-1 Therapie auf synergistische Weise unterstützen. Gleichzeitig konnte allerdings durch die Therapie mit VEGFR-Blockade allein eine vermehrte Metastasierung in der Leber beobachtet werden. Auch *in vitro* hat sich gezeigt, dass die Blockade des VEGF-Rezeptors einen invasiveren Phänotyp induzierte. Die Tumorzellen der Mäuse, welche Lebermetastasen aufwiesen, zeichneten sich durch eine erhöhte Expression des ANG-2 Rezeptors CD29 (Integrin-β1) aus, sowohl in Tumorzellen aus dem primären Lungentumor als auch in solchen, die aus der Lebermetastase isoliert wurden. Diese Ergebnisse lassen zu dem Schluss führen, dass die VEGF-Rezeptor Inhibition über eine Hochregulation des Integrins CD29 einen invasiveren Tumor Phänotyp induzieren könnte, der sich *in vivo* in einer gesteigerten Lebermetastasierung manifestiert. Zur Unterbrechung dieser malignen Signalkaskade konnte der CD29-Ligand ANG-2 durch einen Antikörper blockiert werden, was *in vivo* zu einer signifikanten verminderten Lebermetastasierung und somit zu einem signifikant verbesserten Überleben der Mäuse mit SCLC führte (*under revision*).

SUMMARY

Among the various lung cancer subtypes, small cell lung cancer (SCLC) accounts for about 15% of diagnoses. This subtype is characterized by an extraordinarily rapid progression and a particularly poor prognosis. SCLC is treated with platinum-based chemotherapy which can be extended by immunotherapy in the form of Atezolizumab, a PD-L1 blocking antibody, since 2018. A major challenge in the treatment of SCLC is its ability to evade the tumor-specific immune response. The general aim of immunotherapy is to prevent this mechanism so that the immune system can effectively fight the tumor again. However, especially in the treatment of SCLC, immunotherapeutic effects may be limited, among other factors, by an insufficient immune cell infiltration of the tumor. This condition is in turn caused by the dysfunctional vascular architecture of the tumor, which is based on high levels of the pro-angiogenic factors such as the vascular endothelial growth factor A (VEGF-A) and Angiopoietin-2 (ANG-2). In order to counteract the tumor-promoting effects, we extended the immunotherapy with an anti-angiogenic therapy in our study.

In my thesis it could be demonstrated that the combination of PD-1, ANG-2 and VEGFR blockade significantly increased the survival of SCLC-bearing mice. Thereby, the blockade of ANG-2 and VEGFR could support the anti-PD-1 therapy in a synergistic way. At the same time, however, increased metastasis in the liver was observed as a result of therapy with VEGFR blockade alone. Also *in vitro* it has been shown that blocking the VEGF receptor induces a more invasive phenotype. Tumor cells of mice showing liver metastases were characterized by increased expression of the ANG-2 receptor CD29 (integrin-β1), both in tumor cells from the primary lung tumor and in those isolated from the liver metastasis. Based on these results we suggest that VEGF receptor inhibition may induce a more invasive tumor phenotype via upregulation of integrin CD29. In order to interrupt this signaling cascade, the CD29 ligand ANG-2 was blocked by an antibody, which led to a significant reduction of liver metastasis *in vivo* and finally lead to a significantly prolonged survival of mice suffering from SCLC (*under revision*).

2 INTRODUCTION

2.1 SMALL CELL LUNG CANCER

2.1.1 Epidemiology

Cancer is the second most common cause of death after cardiovascular diseases in Germany [1]. It is estimated that in 2019 500,000 people died of cancer in Germany and the number is projected to increase to 600,000 in 2030. The German Federal Government took this as an opportunity to initiate the “National decade against cancer”, highlighting the rising importance of research on this challenging disease.
Lung cancer is the second most common cancer in men and the third most common in women in Germany. At the same time lung cancer is responsible for the most cancer related deaths in men and second most in women. The median age at diagnosis is 70 years and the 5 year survival rate is particularly poor with only around 13-19% [2].

Regarding to the histology the current World Health Organization classification of lung cancer distinguishes Non-small cell lung cancer (NSCLC), Small cell lung cancer (SCLC) and Carcinoids. NSCLC can be further subgrouped into adenocarcinoma, squamous cell carcinoma and large cell carcinoma, which includes tumors bearing neuroendocrine differentiation, known as Large Cell Neuroendocrine carcinoma (LCNEC) [3]. SCLC accounts for around 20% of lung carcinomas in Germany [2]. It is the most aggressive subtype of lung cancers and patients suffering from it are confronted with a devastating prognosis as the 5 year survival rate is less than 7% [4]. The majority of SCLC patients are smokers or ex-smokers and tend to have a variety of comorbidities including the pulmonary and cardiovascular system. The decline in cigarette smoking in the western world has been associated with a reduced incidence of SCLC over the recent decades, the prognosis for patients however has not improved during this period [5].

2.1.2 Clinical presentation

Besides the typical symptoms of malignant diseases such as fever, weight loss and night sweats, most patients present with lung-specific symptoms including coughing, dyspnea and signs of superior vena cava syndrome in cases of advanced tumor spread [6]. A special aspect of SCLC, distinguishing it clearly from other tumors of the lung, is the frequent occurrence of paraneoplastic syndromes [7]. These disorders arise from an impaired secretion of peptides and hormones by the tumor cells (endocrine paraneoplastic syndrome) or from immune cross-reactivity between the tumor and surrounding regular tissue (neurological paraneoplastic syndrome) [8]. In certain instances, the identification of these distinct disorders can lead to the detection of the responsible, otherwise clinically occult tumor at an early and treatable stage.

Around 10% of SCLC patients suffer from syndrome of inadequate antidiuretic hormone secretion (SIADH), that is defined as an increased secretion of antidiuretic hormone and is diagnosed through hyponatremia in blood tests [9]. About 5% of SCLC patients exhibit elevated secretion of adrenocorticotropic hormone (ACTH), which leads to the development of Cushing's disease due to the high steroid blood levels [10]. Besides these endocrine paraneoplastic syndromes, the neurological Lambert-Eaton myasthenia syndrome appears to be typical for SCLC patients. The disorder manifests as muscle weakness (myasthenia) of the extremities [11].

2.1.3 Pathology

2.1.3.1 Classification

Like any other tumor, SCLC can be staged according to TNM classification as defined by the Union of International Cancer Control (UICC). In fact, an older and simplified classification is widely used for staging, mainly due to its simplicity and clinical utility. This clinicopathological system distinguishes between limited stage (LS) and extensive stage (ES) disease [12]. LS is characterized by a tumor volume that does not exceed one radiation portal; any tumor, that does not meet this criterion and has already metastasized is defined as ES disease. The very limited stage (VLS) was subsequently added as a subgroup of the LS disease for the very rare case that no lymph node dissemination has occurred. This stage only applies to incidentally detected suspicious pulmonary foci that are identified as SCLC in the pathological examination after surgical resection [6]. Despite or rather because of the simplicity of this classification and the resulting inaccuracies, it is recommended to classify according to TNM. A retrospective analysis of 8000 SCLC patients revealed that the prognosis becomes more accurate when more stages are used [6]. The two classification systems can be easily converted into each other. LS can be subgrouped to TNM stage I-III and ES complies with TNM stage IV [6]. As the tumor grows very fast and metastasizes early approximately two third of the patients are being diagnosed at ES (TNM IV) [13]. Metastatic lesions form predominantly in the liver and central nervous system [12].

2.1.3.2 Molecular Pathology of SCLC

SCLC describes a group of tumors characterized by a neuroendocrine differentiation displayed through expression of neuroendocrine markers (chromogranin A, CD56/NCAM, synaptophysin), short doubling time and a high growth fraction represented by high expression levels of Ki67 in immunohistochemistry [14].

Thomas and Pommier postulate that the hallmarks of SCLC, that enable tumor growth and metastatic dissemination, are “sustained proliferation, resistance to apoptosis, unlimited replicative potential, genomic instability and evasion of growth suppressors” [15]. As SCLC

shows the strongest association with cigarette smoking among all lung cancer subtypes the tumors consequently harbor genomic instability and an exceptionally high load of somatic mutations, also referred to as 'tumor mutational burden' (TMB) [16]. A comprehensive genomic analysis of SCLC tumor samples revealed a universal biallelic inactivation of *RB1* and *TP53* [17]. *RB1* and *TP53* are tumor suppressor genes, which play a major role in limitation of cell proliferation. Inactivation of RB1 allows cells to enter into the cell cycle resulting in uncontrolled cell proliferation. P53, also referred to as 'guardian of the genome', is physiologically upregulated upon DNA damage and induces cell cycle arrest and apoptosis. Upon inactivation of *TP53* the inhibition of cell proliferation is abrogated and resistance to apoptosis is established, which is a relevant hallmark for tumorigenesis, as described above [18]. Other than that, amplified copy numbers of members of the *MYC* family can frequently be identified [19]. These transcription factors act as oncogenes upon gain of function and lead to sustained cell proliferation [15].

SCLC features an intratumoral heterogeneity that involves neuroendocrine (NE) and non-NE tumor cells [20]. NE epithelial cells in the upper bronchioles are considered to be the major cell of origin in SCLC development [21]. Additionally, Surfactant protein C (SPC) expressing alveolar type II cells are suggested as the non-NE tumor-origin cells [21]. Notch signaling appears to be the main regulator of the NE differentiation [17,20]. One of the main downstream targets in the Notch signaling axis is Achaete-scute homolog 1 (ASCL1) [22]. ASCL1 is a major player in the induction of "small-cell-ness" and was identified in both SCLC and non-SCLC featuring NE markers [23,24]. Notch activation results in degradation of ASCL1 and thus it was demonstrated that Notch activation can transform NE SCLC cells into slow growing non-NE cells, limiting the tumor growth [17,25]. These non-NE cells are relatively resistant to chemotherapy and may support the surrounding NE cells in their growth - in essence, they are pro-tumorigenic [25]. Hence, Lim *et al.* postulate that Notch signaling features both tumor-promoting and tumor-suppressing capabilities [25]. In around 25% of SCLC patients *NOTCH* inactivation was found in a genomic profiling, highlighting the importance of this pathway [17]. Delta-like protein 3 (DLL3) is an inhibitory Notch ligand that is regularly upregulated on NE SCLC cells, making it a potential specific target [26]. Patients suffering from ES SCLC were treated with DLL3 targeted antibody-drug conjugate Rovalpituzumab Tesirine (Rova-T) in clinical trials [27]. Even though initial results showed promising effects, further clinical evaluations are required and several Phase I clinical trials are underway [27].

The immunohistological evaluation of PD-L1 expression on tumor cells can be the basis for the prediction of the therapeutic success of PD-1/ PD-L1 blockade. In NSCLC, the 'Cologne-Score' for the objective assessment of PD-L1 expression on tumor cells has proven to be a suitable method to identify patients who are more likely to benefit from a targeted PD-1/ PD-L1 blockade [28,29]. For SCLC, expression levels of PD-L1 on tumor cells were characterized in

patient samples by the use of immunohistochemistry (IHC), as well [30]. Depending on the investigating study, PD-L1 was expressed in >1% of the tumor cells in 6 to 15% of SCLC cases [31-33].

2.1.4 Standard of care treatment

Over the last three decades neither the life expectation for a patient diagnosed with SCLC nor the therapy options have changed [27]. The therapy is based on staging as VLS, LS or ES disease: VLS and LS are treated in a curative intention whereas ES disease displays a palliative situation, where complete curation is not aimed for. VLS is the only stage, in which surgery is regularly performed, followed by adjuvant chemotherapy with Cisplatin and Etoposide. Due to the presence of lymph node dissemination in LS disease, surgery is not an option and the patients are treated with 4-6 cycles of Cisplatin and Etoposide with additional simultaneous radiation. Tumor spread that exceeds the area of one radiation portal is defined as ES. Consequently, radiation cannot be performed and patients are only treated with Cisplatin and Etoposide in a palliative intention. Because the central nervous system (CNS) is a predominant site for metastasis formation in SCLC, prophylactic cranial irradiation (PCI) is regularly performed at any tumor stage after completed chemotherapy, depending on the ECOG scale of performance status [34].

The chemotherapy with Cisplatin and Etoposide provides mostly good initial response rates, as the SCLC cells proliferate very fast; however it is usually followed by an early relapse [15]. Second line therapy consists of chemotherapy with a different agent, usually Topotecan, and radiation of the tumor lesions, if the radiation portal is not too large [34]. The first major change in SCLC treatment was the recent inclusion of the monoclonal anti-PD-L1 antibody Atezolizumab to the first line therapy of certain SCLC patients [35]. Patients, who suffer from ES disease and in whom no CNS metastases were detectable are treated with Atezolizumab in combination with Cisplatin and Etoposide followed by Atezolizumab maintenance therapy [35]. In contrast, for NSCLC treatment various new therapy options are available, as NSCLC harbors several mutations that can be exploited through targeting them therapeutically. Targeted therapies facing, for example, *EGF-R* or *EML4-ALK* mutations provide significantly improved survival rates [16].

2.2 IMMUNOTHERAPY

2.2.1 Principles of immunotherapy

Immunotherapy arose in the last years as a promising therapeutic tool in several cancer entities [36-38]. The cellular immune system is capable of fighting foreign, dysfunctional and degenerated cells and thus can also eliminate cancer cells. Effective immune responses

require sufficient activation of participants in the cellular immune system. Professional antigen presenting cells (APC) can recognize, capture and process neoantigens of degenerated cancer cells before they leave the tumor site and reach regional lymph nodes. Regional lymph nodes are the place where APCs present the processed tumor antigens to Cytotoxic T-Lymphocytes (CTL). The presentation takes place via Major Histocompatibility Complex (MHC) II on the surface of APCs, which binds to the T-cell receptor (TCR) of Cytotoxic T-Lymphocytes and can thus activate and prime the CTLs for the specific tumor antigens [39]. The activation is only fulfilled upon costimulatory binding of CD28 on T-cells and CD80/86 on APCs. The next step for the activated effector T-cells is to infiltrate the tumor site again and to recognize specific tumor antigens, which are presented by the tumor cells via MHC I. Upon interaction between the TCR and MHC I cytotoxic factors including granzymes and perforins are secreted by the CTL resulting in cell death of the tumor cell [40].

Cytotoxic T-lymphocyte-associated protein 4 (CTLA4) and programmed cell death receptor 1 (PD-1) are located on the surface of immune effector cells, most notably T-cells and they are known as inhibitory immune checkpoint receptors. Immune checkpoint receptors are physiologically expressed on T-cells to prevent excessive and harmful inflammation and to maintain the immune tolerance to auto-antigens [41]. CTLA4 competes with CD28 to bind CD80/86 during T-cell activation and can therefore attenuate the T-cell function in a very early stage. PD-1 is involved in another part of T-cell immunity: Binding of the predominant ligand PD-L1 to PD-1 has several effects including apoptosis of T-cells, T-cell exhaustion and increased secretion of the immunosuppressive IL-10 [42]. PD-L1 is expressed on various cell types including tumor cells, dendritic cells, macrophages, fibroblasts and T-cells [42,43]. PD-L1 expressing tumors hijack this pathway to prevent the immune response against the tumor antigens, which are recognized by T-cells as foreign and thus play a major role in the immune evasion of the tumor [44-46]. There are two major pathways which are known to regulate the PD-L1 expression levels on tumor cells. Firstly, PD-L1 expression can be upregulated by constitutive activation of oncogenic signaling: Loss of tumor suppressor phosphatase and tensin homolog (PTEN) and the consecutive activation of the phosphatidylinositol-3-OH kinase (PI3K) pathway was shown to increase the PD-L1 expression in glioma [47,48]. Secondly, it was shown that activation of the oncogenic anaplastic lymphoma kinase (ALK) induced PD-L1 upregulation on lymphoma cells through increased expression of the transcription factor STAT3 [49].

Immune checkpoint receptors like PD-1 are physiologically expressed on T-cells so that harmful inflammation can be attenuated upon PD-L1 binding. Therefore, proinflammatory cytokines such as IFN-g, which is secreted by T-cells during inflammation, can upregulate expression levels of immunosuppressive PD-L1 [50,51]. Analogously the secretion of IFN-g in the

inflammatory tumor microenvironment can then upregulate the PD-L1 expression on tumor cells [51].

The aim of immunotherapy is to prevent the neutralization of the effector T-cells by the tumor so that the immune system can effectively fight the tumor again [52]. In a therapeutic approach this is achieved through the interruption of the PD-1/ PD-L1 signaling pathway by applying monoclonal antibodies such as nivolumab and pembrolizumab, which block PD-1 or PD-L1 respectively and thus prevent inactivation of the T-cells through the tumor and the tumor micromilieu [53]. PD-1/ PD-L1 cancer immunotherapy is used to treat several tumor entities with a focus on lung cancers, gastrointestinal cancers and melanoma, based on the number of trials [54].

However, the antitumor effect of immunotherapy is limited due to resistances: Resistances are categorized into primary and acquired resistance. Whereas primary resistance is defined as the absence of therapy response from the outset on, acquired resistances occur under ongoing therapy after an initial response was achieved [55]. The recognition of tumor specific mutant antigens is required to activate the immune system and in particular the T-cells for the anti-tumor action [56]. Primary resistances mainly occur when the tumor prevents recognition of such antigens by T-cells. This can be achieved through two approaches. First of all, a sufficient immune response cannot be obtained if the tumor does not express any mutant antigens [57]. Secondly, an analogous situation is caused by the lack of antigen presentation via Major Histocompatibility Complex (MHC) on the tumor cell surface [58]. Acquired resistances, however, develop in the process of ongoing therapy: On the one hand, they can be a consequence of impaired T-cell function and / or recognition. On the other hand, the clonal selection of specific mutations of the cancer cells can cause the tumor's escape from the immune system [55]. Interferons (IFN) are secreted at high levels by the T-cells during anti-tumor activity. IFN-g signaling is known to cause resistances against immunotherapy by impairing the T-cell function through upregulation of PD-L1 on the tumor cells [59]. Another way that leads to the induction of acquired resistances against immunotherapy is the development of mutations, which facilitate the cancer cells' immune evasion. As described above genetic alterations of PTEN and ALK can lead to immune evasion through PD-L1 upregulation [47-49]. It was further shown that the mitogen-activated protein kinase (MAPK) impairs anti-tumor effect of T-cells [60]. The lack of tumor antigen presentation via MHC-I was previously described as primary resistance above [58]. However, in fact it can also play a role in acquired resistance as the loss or downregulation of MHC-I upon ongoing immune checkpoint blockade is regularly described in several human tumor entities [61]. Exemplary for this is the acquisition of resistance to immune checkpoint blockade in melanoma patients through loss of the beta-2-microglobulin (B2M) gene, an essential component of MHC class I antigen presentation [62,63].

2.2.2 Immunotherapy in SCLC

SCLC harbors a high load of somatic mutations, also referred to as high tumor mutational burden (TMB) due to the strong coherence between cigarette smoking and SCLC development [17,19,64]. Concerning immunotherapy, high TMB was identified as a potential positive predictor for the effectiveness of immune checkpoint blockade [65]. Hellmann *et al.* reported that the objective response rates to Nivolumab (anti-PD-1) ± Ipilimumab (anti CTLA-4) immunotherapy was enhanced in patients suffering from SCLC with a high TMB compared to patients with a low TMB [66]. Nevertheless, immunotherapy did not show as promising effects in SCLC patients as it did in other solid tumors, in spite of the supposedly favorable conditions mentioned above. This may be due to the fact that SCLC is characterized by a highly immunosuppressive phenotype. The level of tumor infiltrating lymphocytes is low and immunosuppressive myeloid cells are a common component of the TME [67]. The frequent lack of MHC I mediated antigen presentation is also contributing to an impairment in immune response [68]. Furthermore, the PD-L1 expression of SCLC cells is rather low particularly in comparison to NSCLC, which impedes therapeutic blockade of PD-1/ PD-L1 axis [69].

In a clinical study of the year 2016 patients suffering from SCLC diagnosed as both limited and extensive stage, who had a relapse after initial platinum based chemotherapy were treated with either Nivolumab (aPD-1) or Nivolumab together with Ipilimumab (aCTLA4). The combination of Nivolumab and Ipilimumab showed a significantly more effective antitumor activity than Nivolumab monotherapy did [70]. The most recent clinical study included patients suffering from extensive stage SCLC who were to receive first line therapy. In this setting, two therapy groups were implemented, being either platinum-based chemotherapy alone or the same chemotherapy together with the monoclonal antibody targeting PD-L1, Atezolizumab. The addition of Atezolizumab to the standard chemotherapy significantly improved the overall and progression-free survival and was therefore recently included to the first line therapy. This adaption was the first major change to SCLC treatment in decades [35]. Although the addition of PD-L1 blocking antibody Atezolizumab improved the survival rates in a significant way, the absolute increase of survival time is still unsatisfying: The rate of overall survival at 12 months was 51.7% in the Atezolizumab group versus 38.2% in the Placebo group [35]. These data underline in general the critical need for further improvement of immunotherapy in SCLC [71]. As mentioned above, SCLC is characterized by an immunosuppressive TME, limiting the efficacy of immunotherapy. One of the key factors contributing to this condition is the dysfunctional vascular architecture of the tumor, which hinders proper passage of immune cells to the tumor and thus to the site where they exert their function [72,73].

2.3 TUMOR ANGIOGENESIS

2.3.1 Principles of tumor angiogenesis

The induction of angiogenesis is one of the six hallmarks of cancer, which are acquired during the development of human tumors [74]. Like any other organ, tumors need blood supply to satisfy their demand for oxygen and nutrients [75]. Precancerous noninvasive lesions are encapsulated and do not feature any proper interconnection to the physiological blood vessels yet. The tumor progression from benign to malignant invasive stage is typically associated with induction of angiogenesis and connection to surrounding vessels – the so called 'angiogenic switch' [76]. The term angiogenesis, which describes the vessel sprouting originated from preexisting vessels, is to be distinguished from vasculogenesis, the *de novo* vessel formation [75]. The key driver for angiogenesis is hypoxia, regularly occurring in solid tumors [77,78]. Hypoxic cancer cells secrete vascular endothelial growth factor A (VEGF-A) which binds to its receptor VEGF – receptor 2 (VEGFR2) on the surface of endothelial cells. In the following this leads to the transformation of ECs towards so called 'tip cells': The endothelial cells form filopodia, become motile and sprout towards high gradients of soluble VEGF-A [79,80]. Another angiogenic factor essential for vessel sprouting is Angiopoietin-2 (ANG-2) as it mediates the destabilization of endothelial cell junctions [80].

Tumor vessels are characterized by an abnormal architecture including poorly interconnected endothelial cells, uneven and loose pericyte coverage and irregular basal membrane structure. Given these circumstances, a dysfunctional network is generated that facilitates the intravasation and dissemination of tumor cells [75,81]. Various cells in the tumor microenvironment are capable of angiogenic signaling. Monocytes extravasate towards the tumor site and differentiate to tumor-associated macrophages (TAMs). TAMs exert a proangiogenic profile as they possess the capacity to secrete VEGF in human cancers [82] and can thus cause angiogenesis and vascular permeability, leading to an increase of the tumor's invasive properties [83]. A positive correlation between the number of TAMs at the tumor site and the tumor's vascular density can be observed [84,85]. Neutrophils, MDSCs and immunosuppressive T_{reg} cells are also associated with proangiogenic signaling [80,86].

Tumor vasculature and the endothelium itself are able to inhibit immunosurveillance at the tumor site as they regulate the leukocyte trafficking. T-cells extravasate through a multistep process that involves binding to cell adhesion molecules like intercellular cell adhesion molecule 1 (ICAM1) and vascular cell adhesion molecule 1 (VCAM1) [87]. Leukocyte extravasation from tumor vessels is suppressed as angiogenic factors downregulate the expression and diminish the functionality of ICAM1 and VCAM1 on ECs hence limiting the extravasation to the tumor site [80,88,89]. Consistent with the aforementioned, Wu *et al.* confirmed an increased expression of ICAM1 and VCAM1 in tumor vessels upon treatment with VEGF-

A neutralizing antibody Bevacizumab, leading to an augmented immune recognition in the TME [90].

2.3.2 Rationale to combine immunotherapy with antiangiogenic treatment

An approach to overcome immunosuppressive mechanisms that are limiting the efficiency of immune checkpoint blockade (ICB) is the combination of immunotherapy with antiangiogenic treatment [91]. Antiangiogenic therapy was shown to generate a more favorable tumor microenvironment, improve drug delivery to the tumor site, and augment T-cell infiltration, thereby providing the basis for a successful immunotherapy [92-94]. Several preclinical and clinical studies have addressed this aspect and combined immunotherapy with VEGF blockade and favorable effects were observed [95-99].

In an autochthonous SCLC mouse model Meder *et al.* showed that treatment with anti-PD-L1 antibody increased both progression-free and overall survival [96]. The combination with additional anti-VEGF antibody was shown to have a significant benefit over monotherapy with anti-PD-L1 and it was demonstrated that combination therapy of anti-VEGF and anti-PD-L1 exerted its effects not in an additive but in a synergistic way. It is further of note, that the OS survival rate was higher in mice treated with anti-PD-L1/ anti-VEGF combination therapy than in mice treated with the standard chemotherapy consisting of Cisplatin and Etoposide. In a next step, the effects of the different therapy options on the tumor-associated T-cells were investigated. Combination therapy was found to be superior to monotherapy with either anti-VEGF or anti-PD-L1 in terms of $CD4^+$ and $CD8^+$ T-cell infiltration to the tumor site. Ongoing treatment with anti-PD-L1 led to an exhausted phenotype of $CD8^+$ T-cells, characterized by increased expression of immune checkpoint receptors PD-1 and TIM-3, that represents a potential mechanism of adaptive resistance to immunotherapy. This exhausted state was rescued through concomitant blockade of VEGF signaling, which may indicate how the combination synergistically prolonged the survival [96]. Despite these encouraging results, which support the rationale that ICB should be combined with anti-angiogenic therapy, emerging evidence suggests that VEGF blockade may result in a more invasive tumor phenotype: A study by Volz *et al.* provides evidence that the inhibition of tumor VEGFR2 induces tumor cell invasion and thus promotes metastasis formation in Non-small cell lung cancer [100].

Like established before, ANG-2 is an important factor in tumor angiogenesis regulation besides VEGF. ANG-2 blockade in mouse tumor models inhibited tumor growth, “often more prominently so when combined with anti-VEGFA drugs […], suggesting that VEGF-A and ANGPT2 function nonredundantly during tumor angiogenesis” [94]. The therapeutic blockade of ANG-2 was further shown to impede metastatic growth in several mouse models of different tumor entities [101-104]. Schmittnaegel *et al.* showed that combined ANG-2 and VEGF-A blockade

is a potent stimulus for the innate and the adaptive immune system and therefore induced antitumor immunity which was further enhanced by additional PD-1 blockade [94].

In order to suppress the entire angiogenic signaling axis, including possible compensatory pathways via ANG-2 after VEGF blockade, and to abrogate development of a more invasive phenotype through VEGF blockade, the approach of our project is to combine anti-ANG-2 treatment with a combination therapy of VEGF blockade and ICB.

2.4 STUDY AIMS

A) Characterization of the immunosupportive role of targeting ANG-2 and VEGF-A combinded with PD-1 blockade in SCLC immunotherapy.

B) Deciphering the effects of ANG-2 and VEGF-A signaling on the invasiveness of SCLC.

3 MATERIAL AND METHODS

3.1 MATERIAL

3.1.1 Murine cell lines

Murine cells RP157.8 (derived from liver metastasis of SCLC-bearing mouse), RP145.5 (derived from primary lesion of SCLC-bearing chemotherapy refractory mouse) and RP254.1 (derived from primary lesion of SCLC-bearing chemotherapy naïve mouse) were used and cultivated with GlutaMax^{TM} -I + 10% FBS + 50µg/ml Penicillin/Streptomycin.

Further, murine SCLC cell lines were used, derived from primary *Rb1* and *Tp53* knockout driven SCLC lung tumors of mice, which had previously been genetically modified (VEGF-A knockout) using CRSPR Cas9 by members of the research group I am affiliated with (VEGFA_KO_1 and VEGFA_KO_2).

3.1.2 Antibodies

3.1.2.1 Flow cytometry antibodies

All antibodies are murine-specific.

Antibody	Flow Channel	Flow Name	Dilution	Supplier	Isotype	Clone
PD-L2	FL1	FITC	1/200	Invitrogen	Rat IgG2a, k	122
CD8a	FL1	FITC	1/200	Biolegend	Rat IgG2a, k	53-6.7
ItGaV	FL1	FITC	1/200	MyBioSource	Rat IgG2a, k	
Galectin-9	FL2	PE	1/100	Biolegend	Rat IgG2a, k	108A2
Tie-2	FL2	PE	1/100	Biolegend	Rat IgG1,k	TEK4
Neuropilin-1	FL2	PE	1/100	Biolegend	Rat IgG2a, k	3E12
EPCAM	FL3	PE/Dazzle	1/100	Biolegend	Rat IgG2a, k	G8.8
CD4	FL3	PE/Dazzle	1/100	Biolegend	Rat IgG2b, κ	GK1.5
CD61	FL4	PerCP/Cy5.5	1/100	Biolegend	Hamster IgG	2C9.G2
TIM-3	FL4	PerCP/Cy5.5	1/100	Biolegend	Rat IgG1,k	RMT3-23
VEGFR2	FL4	PerCP/Cy5.5	1/100	Biolegend	Rat IgG2a, k	89B3A5
PD-L1	FL5	PE-Cy7	1/100	Biolegend	Rat IgG2b, κ	10F.9G2
CD49e	FL5	PE-Cy7	1/100	Biolegend	Rat IgG2a, k	5H10-27
VEGFR2	FL5	PE-Cy7	1/100	Biolegend	Rat IgG2a, k	AVAS12
CD69	FL5	PE-Cy7	1/100	Biolegend	Armenian Hamster IgG	H1.2F3
NCAM	FL6	APC	1/100	R&D systems	Rat IgG	
PD-1	FL6	APC	1/100	Biolegend	Rat IgG2a, k	29F.1A12
CD3	FL7	AF700	1/200	Biolegend	Rat IgG2b, κ	17A2

VEGFR1	FL7	AF700	1/20	R&D systems	Rat IgG2b, κ	
CD45	FL8	APC/Cy7	1/100	Biolegend	Rat IgG2b, κ	30-F11
CD29	FL9	Pacific Blue	1/100	Biolegend	Armenian Hamster IgG	HMb1-1
H2kB	FL9	Pacific Blue	1/200	Biolegend	Mouse IgG2a, k	AF6-88.5
Zombie	FL10	Aqua	1/200	Biolegend		

3.1.2.2 Western blot antibodies

Antibody	Dilution	Supplier	Product number
p-FAK Tyr397	1:1000	Cell Signaling	3283
FAK	1:1000	Cell Signaling	D2R2E
p-SRC Tyr416	1:500	Cell Signaling	2102
SRC	1:1000	Cell Signaling	36D10
β-actin	1:3000	MP Biomedicals	C4

3.1.3 Stimulating reagents

All reagents are murine-specific

Name	Supplier
Angiopoietin-2	R&D Systems
CD28	BD Pharmingen
CD28 IgG	BD Pharmingen
CD3 IgG	BD Pharmingen
CD3e	BD Pharmingen
IFN-g	Peprotech
IL-12 p40	Peprotech
IL-15	Peprotech
IL-1a	Peprotech
IL-2	LifeTech
IL-7	Peprotech
IL-9	Peprotech
M-CSF	Peprotech
MIP-1a (CCL3)	Peprotech
MIP-2 (CXCL-2)	Peprotech

VEGF-A	Peprotech

3.1.4 Kits

3.1.4.1 Intracytoplasmic Staining

Intracytoplasmic staining is performed with the kit Beckman Coulter "IntraPrep permeabilization reagent" (Ref. A07803). The active substances are Formaldehyde for fixation and Saponin for permeabilization.

3.1.4.2 RNA extraction

For RNA extraction the Qiagen RNeasy® Mini Kit (LOT 163031352) was used.

3.1.5 Buffers, reagents and devices

- Medium: 500ml RPMI medium 1640 (1x) + GlutaMAX™ -I + 50ml Fresh Bovine Serum + 5ml Pen Strep (5000 units/ml Penicillin + 5000µg/ml Streptomycin)
- Trypsin: 0,05% Trypsin-EDTA (1x), gibco; REF: 25300-054
- DPBS: Dulbecco's Phosphate Buffered Saline (1x), gibco, REF: 14190-094
- ACK Lysing Buffer, Gibco Life technologies, USA (LOT 2037040)
- Trypan Blue Stain (0,4%), Gibco Life technologies, USA
- Dimethyl sulfoxide, C_2H_6OS, PanReac AppliChem, USA (LOT 80014081)
- Centrifuge: Eppendorf® Centrifuge 5702
- Incubator: CO_2 -incubator for cell culture: 37,0°C and 5,0% CO_2 ; company Binder
- Cell culture flask: Cellstar® cell culture flask with 75cm^2 and 175cm^2
- Eppis/ microtubes: SafeSeal microtube 1,5ml
- Cell counting chamber: Neubauer improved counting chamber (depth 0,100mm; 0,0025mm^2) and Trypan Blue Solution, 0,4%.
- FACS: Beckmann Coulter: Gallios® Flow Cytometer; 3 Lasers (405nm, 488nm, 638nm), 10 colors (450nm, 525nm, 550nm, 575nm, 620nm, 660nm, 675nm, 725nm, 755nm)
- FACS analysis software: Beckman Coulter Kaluza® Analysis Software

3.2 METHODS

3.2.1 Cell biological methods

3.2.1.1 Cultivation

The cultivation of the cells takes place under sterile conditions under a workbench Scanlaf Mars 1200 (Labogene, Lillerød, Denmark) and Herasafe® KS 12 (Heraeus, Hanau, Germany).

For sterile handling of the cells pipet tips (VWR, Radnor, USA), Cellstar® cell culture flasks and cell plates (Greiner Bio One, Frickenhausen, Germany) and centrifuge tubes (Corning, New York, USA) were used. Incubation has been carried out in the Binder Series C incubator (Binder, Tuttlingen, Germany) at 37°C, 5% CO_2 and H_2O saturated air. The RPMI medium 1640 (1x) + GlutaMAX™ -I (Thermo Fisher Scientific, Waltham, USA) was used. Once the cells reached a confluency of about 80-90%, they were washed with DPBS before being dissolved with 0,05% Trypsin-EDTA. The trypsination is stopped by adding culture medium and the cell suspension can be split according to the estimated growth rates.

3.2.1.2 Cryoconservation

The cells are washed with DPBS before around $2x10^6$ cells are resuspended with 1ml of Cryoconservation medium (90% FBS + 10% DMSO). The cell suspension is stored in Cryo.S® Tubes (Greiner Bio One, Frickenhausen, Germany) at -80°C. After some time, the tubes are transferred to liquid nitrogen at -196°C.

3.2.1.3 Defrosting cells

Cells are resuspended with medium and washed with DPBS twice before they are resuspended with medium and transferred to a cell culture flask and cultivated.

3.2.1.4 Cell counting

The cells are counted in a Neubauer improved counting chamber using Trypan Blue Solution, 0,4% for the staining.

3.2.1.5 Stimulation of SCLC and immune cells

The cells of interest are seeded into 12 well plates (Greiner Bio One, Frickenhausen, Germany) and incubated overnight before stimulation is undertaken. The stimulating reagents are diluted in medium before they can be added to the existing medium and cells.

3.2.1.6 Fluorescence activated cell sorting (FACS) of tumor and immune cells

In the FACS technique, antibodies bind to the corresponding receptors on the cells. These antibodies are conjugated with fluorochromes, which can be excited by light of a specific wavelength and then emit light of a specific wavelength. This emitted light can then be detected by the device and thus the expression of specific receptors on the target cells can be detected. The cells are counted and seeded onto 12 well plates. The 12 well plates will be full at a number of 200,000 cells per well, so for a 24h stimulation 50,000 cells per well are seeded and the plates are put into the incubator. After 24h the cells are stimulated with the respective antibodies.

After the desired time of stimulation, the cells are collected. Cells growing in suspension are put into centrifuge tubes directly. The cells growing adhesive must be treated with 500µl of trypsin first. The centrifuge tubes are centrifuged at a speed of 0,8rpm for 3 minutes, before the fluid supernatant can be taken off. The cell pellet is resuspended with 1ml DPBS and this suspension will be put into a 1,5ml SafeSeal microtube. These microtubes will then be centrifuged for 3 minutes at a speed of 350rcf and the supernatant will be taken off again. 50µl of the fluorochrome-conjugated antibodies are given to the remaining cell pellet, resuspended and then they are incubated for 30 minutes at a temperature of 4°C.
After this the microtubes are centrifuged again for 3 minutes at 350rcf and the supernatant will be taken away and 100µl of 4% paraformaldehyde is added to the cell pellet and resuspended. This will be incubated for 10 minutes at room temperature in a dark surrounding. After the incubation the microtubes are centrifuged for another 3 minutes with 350rcf and the supernatant will be taken off. The remaining cell pellet must be washed with DPBS before it is resuspended with 200µl DPBS and the content is placed into the prepared FACS tubes.
The FACS analysis is performed with the Gallios® flow cytometer (Beckman Coulter, Brea, USA). The following lasers and fluorochromes were used:

Fluorochrome	**Laser**	**Excitation max.**	**Emission max.**
FITC	488nm	490nm	525nm
PE	488nm	496nm	578nm
PEDazzle™ 594	488nm	566nm	610nm
PerCP-Cyanine5.5	488nm	482nm	690nm
PE-Cyanine7	488nm	565nm	774nm
APC	638nm	650nm	660nm
AF700	638nm	702nm	732nm
APC-Cy7	638nm	650nm	774nm
Pacific Blue	405nm	410nm	455nm
Aqua	405nm	388nm	516nm

Analysis of the FACS data was undertaken by Kaluza® analysis software (Beckman Coulter, Brea, USA).

3.2.1.7 T-cell stimulation

The plate is coated with 200µl per well of CD3 (5µg/ml concentration) or corresponding IgG (5µg/ml concentration) and stored overnight at 4°C.
Spleens of mice were strained through 40µm Nylon cell strainer (VWR, Radnor, USA) and washed with DPBS. For lysis of erythrocytes the splenocytes are treated with 1ml of Ammonium chloride potassium lysis buffer for 10 minutes at room temperature. The cells are

washed with DPBS and counted in the counting chamber. 100,000 cells/ well are seeded in 100µl medium. CD28 (2µg/ml) and IL-2 (40ng/ml) are added to the cells and the cells are treated with Angiopoietin-2 (500ng/ml) and VEGF-A (50ng/ml). The plate is stored in the incubator overnight. After 24 hours FACS analysis is performed as described above.

3.2.1.8 Scratch Assay

75,000 cells per well are seeded into 12 well plates. After 24h a straight scratch is made using a 1000µl pipet tip. The medium containing the abraded cells is taken off and new medium containing the stimulating factors is added. The cells are stimulated with vehicle control (Purified water), Vatalanib (2500ng/ml), or ANG-2 (500ng/ml). Pictures are taken after 0 and 24 hours. The assay is analyzed with respect to the decreasing free area using the program Image J ®.

3.2.2 Molecular biological methods

3.2.2.1 Isolation of mRNA of eukaryotic cells and sequencing

The isolation of mRNA from eukaryotic cells was performed using RNeasy® Mini Kit 50 (Qiagen, LOT 163031352) according to manufacturer's instruction. After isolation the mRNA sequencing was done by the Cologne center for genomics (CCG, University of Cologne) including an initial processing of the generated dataset into a format that could be then further analyzed using Excel®.

3.2.3 Protein-biochemical methods

3.2.3.1 Western Blot

For western blot analysis cells lysates were prepared beginning with digestion of tumor cells using:

- lysis buffer (1 ml lysis buffer (10× Cell Signaling)
- 1× complete protease inhibitor cocktail mini tablet (Roche)
- 1 mM PMSF (Phenylmethylsulfonyl fluoride) (Carl Roth)
- 100 µl phosphatase inhibitor cocktail II (Sigma Aldrich)
- 10mM sodium fluoride (Merck)
- 2µM Sodium pyrophosphate decahydrate (Sigma Aldrich)
- 2µM beta-glycerophosphate (Sigma Aldrich)

The protein-concentrations were determined by a BCA (bicinchoninic acid) Protein Assay (Pierce). For SDS-PAGE (sodium dodecylsulfate polyacrylamide gel electrophoresis) the prepared cell lysates were mixed with NuPage® LDS buffer (4x) and sample reducing agent (10×) (Life Technologies). After that step they were incubated at 80 °C for 10 min and loaded on NuPAGE Bis-Tris Gels 4-12% (Invitrogen, Life Technologies). The samples run for

approximately 90 min at a voltage level of 130V. The separated proteins are transferred onto nitrocellulose Membrane (Amersham Hybond-C Extra) by wet-blotting in a XCell II™ Blot Module (Life Technologies). The nitrocellulose membrane was blocked with Blocking Buffer (4% milk in TBST (tris-buffered saline with tween20)) before it was incubated overnight with the antibodies described above (chapter 2.1.2.2) diluted in blocking buffer. The membrane was washed for 30 minutes with TBST before it was incubated with secondary HRP (horseradish peroxidase) -conjugated antibody 1:3000 in TBST for 1h at room temperature (anti-rabbit-HRP and anti-mouse-HRP antibodies; both from Millipore). After that the membrane was developed on ECL (enhanced chemiluminescence) Hyperfilm with ECL western blot detection System (GE Healthcare). The PTK (protein tyrosine kinase) assay (R&D Systems) was performed according to manufacturer's instructions using 300 µg protein.

3.2.4 Cytokine Array

For the cytokine array, whole blood of mice was incubated for 1h at room temperature in 500Z-Gel Microvettes (Sarstedt) and then centrifuged for 5 min at 20°C with 10,000 x g. 75 µl of harvested serum were analyzed in duplicates. Serum samples of SCLC-bearing mice treated with vehicle control (Vehicle; n=3), VEGFR inhibitor monotherapy (VEGFRi; *n* =3), anti-ANG-2 monotherapy (aANG-2; n=2),and anti-ANG-2 and VEGFR inhibitor combination therapy (aANG-2/ VEGFRi; n=2), anti–PD-1 monotherapy (aPD-1; *n* =3), and anti-ANG-2/VEGFR-inhibitor/anti–PD-1 triple combination therapy (triple; *n* =3) were collected that way. The serum was analyzed for 31 murine cytokine profiles using a 31-Plex Mouse Cytokine Array (Eve Technologies Corporation, Calgary, AB Canada). Cytokine concentrations were clustered using the "Morpheus" software of the Broad Institute (Morpheus, https: //software.broadinstitute.org/Morpheus) hierarchical clustering tool with the parameters Log2(1+X); Min 0; Max 15; Metric: 1- Pearson Correlation [105].

3.2.5 Animal experiments

This study was performed in accordance with FELASA recommendations and with approval of the local Ethics Committee of Animal experiments (84-02.04.2015.A199; 81-02.04.2020.A026). The genetically engineered mouse model of SCLC is driven by a Cre-inducible conditional *Rb1* and *Tp53* knock out [106]. Six-to-twelve-week-old male and female C57BL/6JxFVB/NJx129/Sv mice were anesthetized with Ketamin/Xylazin (100 mg/kg/(body weight) BW Ketamin intraperitoneal/ 0.5 mg/kg/BW Xylazin intraperitoneal) and $3x10^7$ plaque-forming units (pfu) of Adeno-Cre viral vectors was applied intratracheally [107]. Viral vectors were provided by the University of Iowa Viral Vector Core (http ://www.medicine.uiwo.edu/vectorcore). Serial µCT was performed to monitor tumor induction, response to therapy and progression under therapy. Mice were randomized to the six therapy

cohorts before tumor induction. The target lesion diameters at the start of treatment were similarly distributed between the groups.

Twenty weeks after virus inhalation, once a week, mice were anesthetized using 2.5 % isoflurane, and receive a serial µCT scan (LaTheta mCT, Hitachi Alcoa Medical, Ltd). Upon a measurable target lesion ≥ 1 mm in diameter, therapy regimens were started. SCLC cohorts comprised six therapy groups and all therapies were given every 3 days simultaneously: Group 1: vehicle (phosphate buffered saline; PBS); group 2: IgG (corresponding monotherapy IgGs (Southern Biotech, US) diluted in PBS); group 3: anti- ANG-2 (BI836880, Boehringer Ingelheim, Lot.-No. #314A80003, bi-specific nanobody consisting of one domain binding human VEGF-A, one domain binding both human and murine ANG-2 and both domains) with a concentration of 15 mg/kg/BW intraperitoneal per injection; group 4: the VEGFR-tyrosine kinase inhibitor (TKI) Vatalanib (PTK787, Med Chem Express, Lot.-No. #25923, Cat.-No. #HY-12018/CS-0149, diluted in water) with a concentration of 75 mg/kg/BW per oral gavage; group 5: anti-PD-1 (monoclonal antibody RMP1-14, Boehringer Ingelheim, Lot.-No. #640517M2, Cat.-No. #BE0146) with a concentration of 10 mg/kg/BW i.p. per injection; group 6: combined triple combination comprising anti-ANG-2 (15 mg/kg/BW i.p.), Vatalanib (75 mg/kg/BW p.o.) and anti- PD-1 (10 mg/kg/BW i.p.) applied simultaneously.

Tumor response and progress under ongoing treatment was assessed by mouse adapted RECIST criteria v1.1, as published previously [96]. Slice thickness was adapted to 0.3 mm. The first dose was given upon target lesion identification and baseline evaluation, maximum one day before. Response criteria to evaluate the target lesion were maintained regarding diameter fold change. Complete response (CR) referred to a decrease of 100 %, partial response (PR) was indicated upon a >30 % reduction, progressive disease (PD) referred to an increase of >20 % and/or new lung lesions and stable disease (SD) was termed upon a diameter change that did not qualify for PR or PD. µCT data was analyzed using OsiriX-DICOM viewer (aycan Digitalsysteme GmbH).

Overall survival (OS) and progression-free survival (PFS) achieved with the different therapy regimens were analyzed as Kaplan-Meier-Curves and statistically evaluated using Mantel-Cox Prism (GraphPad, V8.0) and the proportional hazard model (R survival package, R Core Team, 3.6.3). Synergy analysis of the triple combination with anti-ANG-2, VEGFR inhibitor and anti-PD-1 was performed with the proportional hazard model. (*under revision*)

4 RESULTS

4.1 TRIPLE COMBINATION OF PD-1/ ANG-2/ VEGFR BLOCKADE SIGNIFICANTLY PROLONGED SURVIVAL OF MICE SUFFERING FROM SCLC

Our group recently showed that the therapy outcome of SCLC-bearing mice was enhanced by the addition of VEGF-targeted treatment to PD-1 blockade [96]. Further, it was shown that blockade of VEGF/VEGFR-signaling induces tumor cell invasion and metastasis [100], which are major components, contributing to the poor outcome of SCLC patients [35]. In order to overcome negative effects of VEGF/VEGFR-targeted therapy in terms of metastatic characteristics, we added anti-ANG-2 antibody to the combination therapy, consisting of VEGFR-inhibitor and anti-PD-1 antibody, for the treatment of SCLC-bearing mice. For this purpose, an autochthonous SCLC mouse model was used, in which specific knockout of *Rb1* and *Tp53* was induced through Cre-adenovirus inhalation. Serial µCT measures were performed to identify target lesions. Upon a measurable target lesion, mice were randomly assigned to the different therapy groups: (i) Vehicle (phosphate buffered saline; PBS); (ii) IgG (corresponding monotherapy IgG); (iii) murine anti-ANG-2 antibody (aANG-2); (iv) inhibitor of VEGFR Vatalanib (VEGFRi); (v) murine anti-PD-1 monoclonal antibody (aPD-1); (vi) combined aANG-2/VEGFRi; (vii) combined aANG-2/ VEGFRi/ aPD-1.

Tumor growth was monitored by serial µCT scans, with the RECIST criteria v1.1 [108] being adapted to the SCLC mouse model. Fold-change of the target lesion diameter was decisive for the evaluation of therapy response. Complete response (CR) indicated a 100% decrease, partial response (PR) referred to a tumor volume shrinkage of < -30%, progressive disease (PD) was defined as increase of tumor volume > +20% and / or new lung lesions, and stable disease (SD) referred to a change in diameter that was not eligible for PR or PD. (*under revision*)

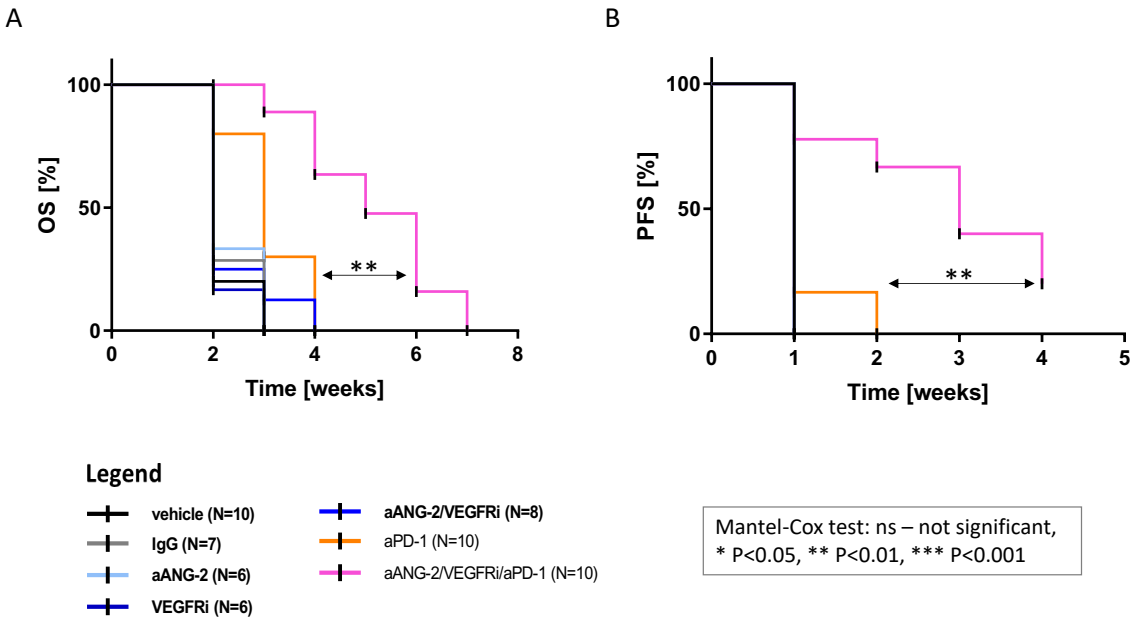

Figure 1: Triple combination of PD-1/ ANG-2/ VEGFR blockade significantly prolonged survival of mice suffering from SCLC.

SCLC-bearing mice were treated with vehicle control (black; n=10), IgG control (grey; n=7), VEGFR inhibitor monotherapy (VEGFRi, dark blue; *n* =6), anti-ANG-2 monotherapy (aANG-2, light blue; n=6), anti-ANG-2 and VEGFR inhibitor combination therapy (aANG-2/ VEGFRi, blue; n=8), anti–PD-1 monotherapy (aPD-1, orange; *n* =10), and anti-ANG-2/VEGFR inhibitor/anti–PD-1 triple combination therapy (triple, pink; *n* =10).

A. + B. OS (Overall survival) and PFS (Progression free survival) were determined from the six therapy groups. Statistical analysis was done using the Prism Mantel–Cox test (**, $p < 0.01$). The analysis was conducted by L. Meder. The experimental procedures and animal care were conducted by L. Meder, C. Otto and medical-technical assistant M. Nill. This figure contains unpublished data that is adapted from *under revision*.

We saw that the combination therapy of ANG-2/ VEGFR/ PD-1 blockade led to a significantly prolonged progression free (PFS) and overall survival (OS) (Figure 1 A, B). Mice treated with the respective monotherapy had an average overall survival of 3 to 4 weeks. This time span was equal to that of mice treated with IgG or vehicle control. Treatment with the triple combination therapy in contrast showed a significantly longer survival of 7 weeks in average. In addition, the triple combination therapy extended the progression-free survival from 2 weeks, observed for the other therapy groups, to 4 weeks. (*under revision*)

Taken together, the therapy of SCLC-bearing mice with a combination of ANG-2/VEGFR/PD-1 blockade resulted in significantly longer PFS and OS compared to anti-PD-1 monotherapy.

4.2 ANG-2 AND VEGF-A DO NOT MODIFY T-CELL ACTIVATION STATUS

In a previous study, Meder and colleagues identified a PD-1/TIM-3 positive exhausted T-cell phenotype upon acquired resistance to anti-PD-L1 treatment in SCLC. This phenotype was ‘rescued’ by therapeutic combination of PD-L1 and VEGF-A blockade [96].

Thus, we hypothesized that T-cell activation, promoted by ANG-2 and VEGF-A, may contribute to the prolonged survival of mice suffering from SCLC. For this purpose, we isolated splenocytes from tumor-bearing and non-tumor-bearing mice and stimulated them with either CD3/CD28 and IL-2 to activate the T-cells or with the corresponding IgG control and IL-2. Additionally, the T-cells were stimulated with either ANG-2, VEGF-A, or a combination of ANG-2 and VEGF-A.

PD-1 is physiologically upregulated upon T-cell activation to oppose exuberant activation and thus PD-1 upregulation can be utilized as a marker for T-cell activation [109]. We saw sufficient $CD4^+$ and $CD8^+$ T-cell activation determined by PD-1 expression upon CD3/CD28 and IL-2 stimulation. However, neither stimulation with ANG-2 and VEGF-A alone nor in combination, modified the level of T-cell activation (Figure 2 A, B).

Consequently, ANG-2 and VEGF-A could not be shown to modify the activation status of T-cells.

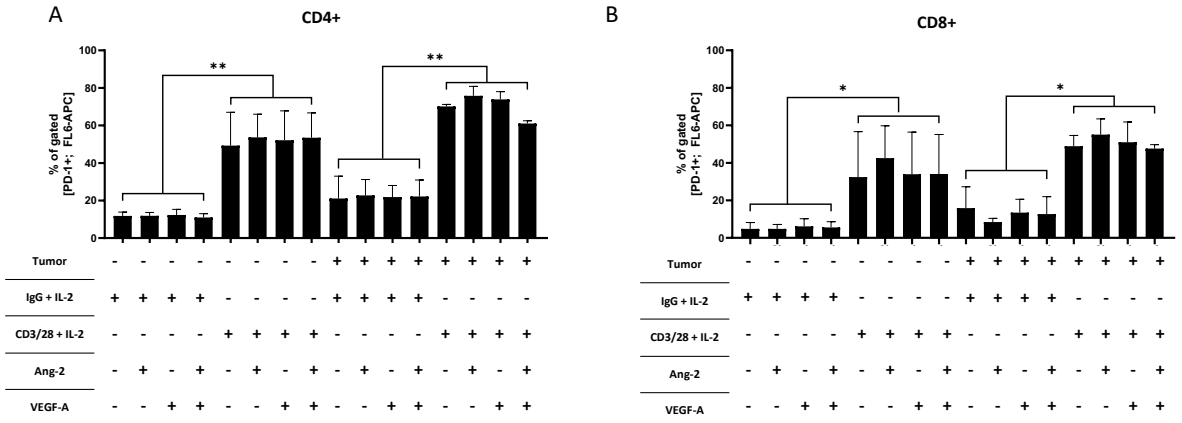

Figure 2: ANG-2 and VEGF-A do not modify T-cell activation status.

Splenocytes from tumor-bearing and tumor-free mice were isolated and stimulated with combinations of CD3/ CD28/ IL-2, IgG control and IL-2, ANG-2, and VEGF-A. Activation status, based on PD-1 upregulation, was examined after 24h of stimulation using flow cytometry. Cell lysates were stained for viable immune cells ($CD45^+$) and nonimmune cells ($CD45^-$). T-cells ($CD3^+$) were identified within the $CD45^+$ gate and were further distinguished between $CD4^+$ and $CD8^+$ T-cells. T-cell activation is assessed based on the increased PD-1 positive population.

A. % of PD-1 positive $CD4^+$ T-cells.

B. % of PD-1 positive $CD8^+$ T-cells.

Statistical analysis was done using the Student's t-test (ns, not significant; *, $p < 0.05$; **, $p < 0,01$;***, $p < 0,001$; error bars, SEM). These experiments were conducted and analyzed by C. Otto.

4.3 TARGETING ANG-2 INDUCES AN IMMUNOSUPPORTIVE CYTOKINE SIGNATURE

As ANG-2 and VEGF-A appeared to have no direct effects on the T-cell activation status we performed a cytokine assay, in order to get a closer look into the therapy associated immune

signature. We analyzed the cytokine levels in the serum of mice, treated with the following therapy regimens: Vehicle control, anti-ANG-2, VEGFR inhibitor, anti-PD-1, combined anti-ANG-2/VEGFRi and combined anti-ANG-2/VEGFRi/anti-PD-1.

In the cytokine array we found the following clusters to be altered upon treatment (Figure 3). Cluster “A” is altered in mice treated with anti-ANG-2 monotherapy and includes the cytokines IFN-g, IL-2, MIP-1a and IL-9. Cluster “B” is composed of IL-7 and IL-15 and is elevated in mice treated with aPD-1 monotherapy. Cluster “C” is referred to the triple combination therapy upon development of resistance and thus progressive disease. It consists of IL-12, IL-1a, M-CSF and MIP-2.

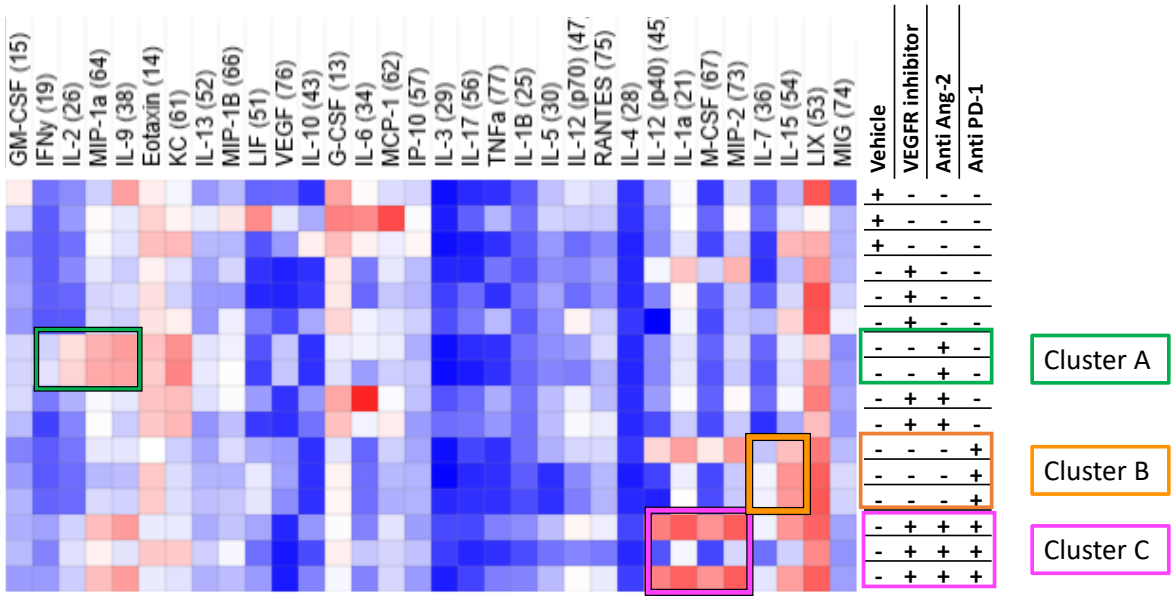

Figure 3: Targeting ANG-2 induces an immunosupportive cytokine signature.

SCLC-bearing mice were treated with vehicle control (Vehicle; n=3), VEGFR inhibitor monotherapy (VEGFRi; *n* =3), anti-ANG-2 monotherapy (aANG-2; n=2),and anti-ANG-2 and VEGFR inhibitor combination therapy (aANG-2/ VEGFRi; n=2), anti–PD-1 monotherapy (aPD-1; *n* =3), and anti-ANG-2/VEGFR-inhibitor/anti–PD-1 triple combination therapy (triple; *n* =3). Upon detection of progressive disease based on µCT measurements and mouse adapted RECIST v1.1 criteria, endpoint analysis was performed and serum probes were cryoconserved for further validation. The serum was analyzed for 31 murine cytokine profiles using a 31-Plex Mouse Cytokine Array (Eve Technologies). Cytokine concentrations were clustered using the Morpheus Broad Institute hierarchical clustering tool. Color code ranges from dark blue (low expression levels) to dark red (high expression levels). The expression levels appear analogous to the color levels.

Based on the therapy we could identify three different clusters of cytokines. Cluster A consists of IFN-g, IL-2, MIP-1a, and IL-9, Cluster B of IL-7 and IL-15 and Cluster C of IL-12, IL-1a, M-CSF, and MIP-2.

The preparation of the samples was conducted by L. Meder and C. Otto. The 31-Plex Mouse Cytokine Array was conducted by Eve Technologies in return for payment of a fee paid by the PI and supervisor of my thesis, Prof. Dr. Dr. Ullrich. The analysis was conducted by L. Meder and C. Otto with the help of S. Borchmann.

4.4 ANG-2 AND VEGF-A DO NOT DIRECTLY AFFECT IFN-G INDUCED PD-L1 EXPRESSION ON SCLC CELLS

Among the cytokines that appeared to be upregulated upon anti-ANG-2 treatment in the serum-cytokine-assay, we found IFN-g. IFN-g is known to be a potent inducer of tumor-associated PD-L1 expression and can thus be part of reduced efficacy of immunotherapy, as described in the introduction [51]. In order to assess the ability of IFN-g to promote PD-L1 expression level on murine SCLC cells of our model, we stimulated the tumor cells with IFN-g for 24 hours before we evaluated the PD-L1 expression in flow cytometry analysis.

Furthermore, we stimulated the tumor cells with different concentrations of all cytokines, contained in the Clusters A, B and C that we identified in the serum-cytokine-assay. We confirmed IFN-g to be a potent inducer of PD-L1 expression while the other cytokines seemed to have no ability to impact PD-L1 expression levels on SCLC cells (Figure 4 A).

As we found IFN-g to promote PD-L1 expression on SCLC cells we wanted to study potential additional effects of ANG-2 and VEGF-A on PD-L1 expression levels. For this purpose we stimulated SCLC cells with combinations of IFN-g, ANG-2 and VEGF-A. Apart from the previously reported ability of IFN-g to induce PD-L1 expression, ANG-2 and VEGF-A seemed to have no additional direct effects on the regulation of PD-L1 expression, neither in monostimulation nor in combination with IFN-g stimulation (Figure 4 B, C).

Conclusively, the IFN-g induced PD-L1 expression on SCLC cells was not directly affected by ANG-2 and VEGF-A.

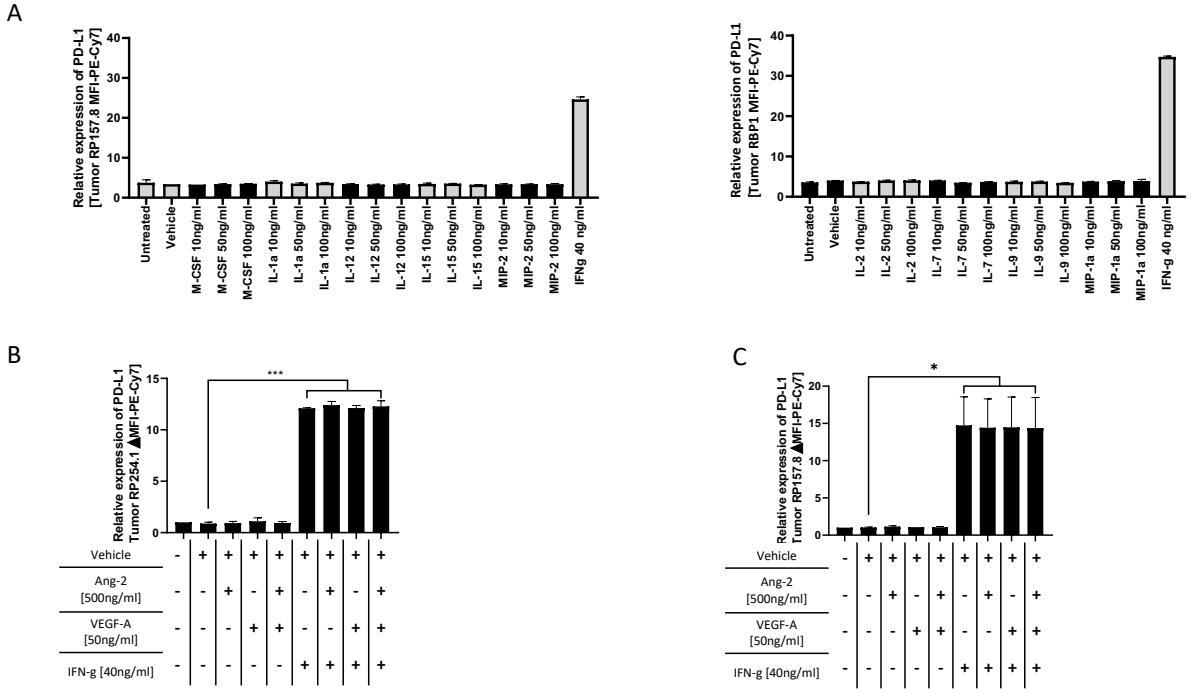

Figure 4: ANG-2 and VEGF-A have no direct effects on IFN-g induced PD-L1 expression on SCLC cells.

A. SCLC tumor cells isolated from murine liver metastasis were stimulated with different concentrations (10ng/ml, 50ng/ml, 100ng/ml) of cytokines revealed in cytokine assay in clusters A,B,C (Figure 3.3) and vehicle control for 24h. Expression levels of PD-L1 were evaluated using flow cytometry.

B. SCLC tumor cells isolated from murine primary lung tumor (RP254.1) were stimulated with combinations of ANG-2 (500ng/ml), VEGF-A (50ng/ml), IFN-g (40ng/ml), and vehicle control for 24h. Expression levels of PD-L1 were evaluated using flow cytometry.

C. SCLC tumor cells isolated from murine liver metastasis (RP157.8) were stimulated with combinations of ANG-2 (500ng/ml), VEGF-A (50ng/ml), IFN-g (40ng/ml), and vehicle control for 24h. Expression levels of PD-L1 were evaluated using flow cytometry.

Statistical analysis was done using the Student *t* test (ns, not significant; *, $p < 0.05$; **, $p < 0,01$;***, $p < 0,001$; error bars, SEM). These experiments were conducted and analyzed by C. Otto.

4.5 ANG-2 RECEPTOR CD29 IS ABUNDANTLY EXPRESSED ON SCLC CELLS AND UPREGULATED UPON METASTASIS FORMATION

We further wanted to decipher the effects of ANG-2 and VEGF-A signaling on tumor invasiveness of SCLC. For this purpose, we examined the expression levels of ANG-2 receptors on SCLC cells, isolated from both primary lung tumor as well as liver metastases. For both we proved that the main ANG-2 receptor TIE2 was not expressed. In turn, various integrins including CD61, CD49 and CD29 were abundantly expressed (Figure 5 A). Exactly this condition with a prominent role of Integrin-β1 (CD29) was described in previous publications to be linked to a more invasive phenotype [110,111].

Based on these results we analyzed the expression levels of CD29 on tumor cells either isolated from primary lung tumors without liver metastasis (L-M) or primary lung tumors with

liver metastasis (L+M) or isolated directly from liver metastasis (M). We found elevated levels of CD29 expression on tumor cells of primary lung tumors upon liver metastasis formation. The CD29 expression was even higher on tumor cells isolated from liver metastases (Figure 5 B). (*under revision*)

In order to assess the downstream signaling of integrin-β1 in SCLC cells we stimulated murine SCLC cells, isolated from liver metastasis, with ANG-2. Western Blot analysis revealed a constant high level of Focal adhesion kinase (FAK) and c-SRC kinase. We further focused on the activating phosphorylation of FAK at Y397 [112] and of c-SRC at Y416 [113]. The Y397 phosphorylation of FAK was increased upon ANG-2 stimulation with a maximum at 20 minutes of stimulation. Also the phosphorylation of c-SRC at Y416 was higher upon ANG-2 stimulation but to a lesser extent than pFAK (Figure 5 C). (*under revision*)

Taken together, SCLC cells exhibit high expression levels of ANG-2 receptor integrin-β1 that are upregulated upon metastasis formation. Further, stimulation of SCLC cells with the integrin-β1 ligand ANG-2 led to activating phosphorylation of the focal-adhesion and c-SRC kinases.

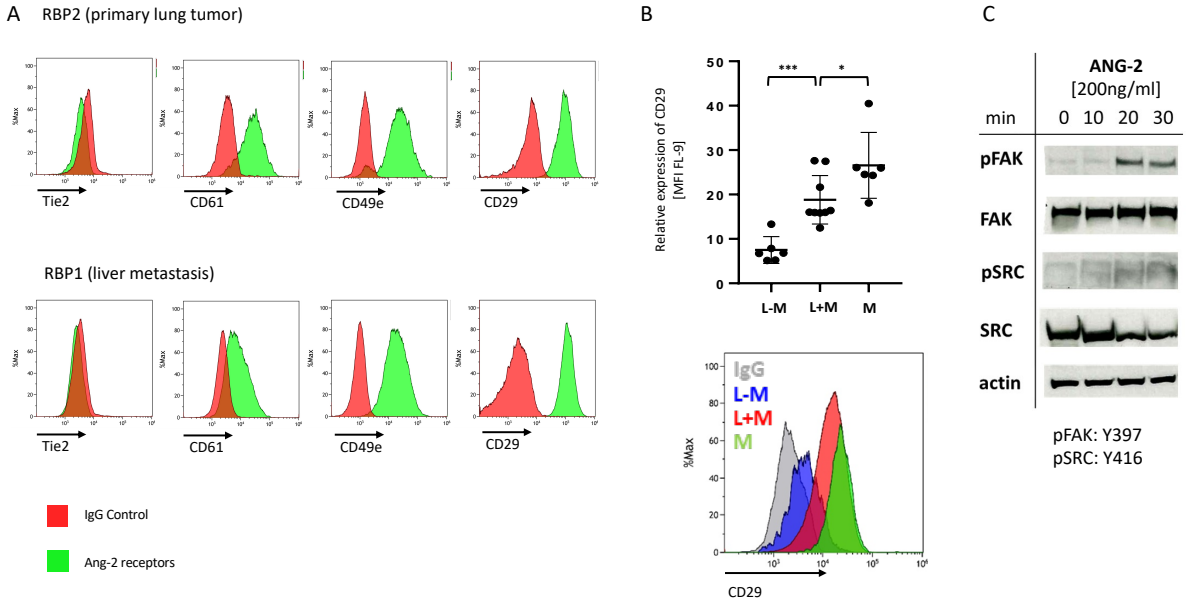

Figure 5: ANG-2 receptor CD29 is abundantly expressed on SCLC cells and upregulated upon metastasis formation.

A. Expression levels of ANG-2 receptors on SCLC cell lines from primary lung tumor and liver metastasis were examined using flow cytometry.

B. Relative expression of CD29 (integrin-β1), determined by mean fluorescence intensity in flow cytometry, on tumor cells isolated from SCLC-bearing mice. L-M: Tumor cells isolated from lungs without visible liver metastasis; L+M: Tumor cells isolated from lungs with visible liver metastasis; M: tumor cells isolated from liver metastasis; IgG: flow cytometry antibody control.

C. Western blot analysis of murine tumor cells isolated from liver metastasis for phosphorylation of FAK at Y397 (pFAK), FAK, phosphorylation of c-SRC at Y416 (pSRC), and SRC. The cells were treated with ANG-2 (200ng/ml) for 10, 20, and 30 minutes. Actin was used as a control (actin).
Statistical analysis was done using the Student's t-test (ns, not significant; *, $p < 0.05$; **, $p < 0,01$;***, $p < 0,001$; error bars, SEM). These experiments were conducted and analyzed by L. Meder and C. Otto. Western blot in figure C was supported by M. Koker. This figure contains unpublished data that is adapted from *"under revision"*.

4.6 VEGFR-I SIGNALING DIRECTLY REGULATES CD29 EXPRESSION AND INDUCES MORE INVASIVE PHENOTYPE *IN VITRO*

Based on a previous publication of our group that describes increased tumor cell invasion in NSCLC upon inhibition of VEGFR2 [100] we analyzed how VEGFR inhibitory treatment may promote invasiveness of SCLC cells. For this purpose we performed a wound healing assay: SCLC cells isolated from liver metastasis were treated with VEGFRi, ANG-2, or vehicle control for 24 hours. The area of migrated cells after 24 hours was significantly higher upon stimulation with VEGFRi compared to vehicle control. The stimulation with the CD29 ligand ANG-2 led to a significantly higher number of migrated cells, as well (Figure 6 A). (*under revision*)
In order to examine more closely whether VEGFR inhibition can modify the expression of integrin-β1 on SCLC cells we simulated the VEGFRi treatment *in vitro*: SCLC cells, isolated from primary lung tumor and liver metastases, were treated with VEGFRi for 14 consecutive days. On days 3, 7, and 14 expression levels of CD29 were measured using flow cytometry. We found increased levels of CD29 after 7 days of constant VEGFRi treatment. The expression levels were even more elevated after 14 days in a significant manner (Figure 6 B). (*under revision*)
Concluding, VEGFR-inhibitor treatment directly regulates the expression of CD29 on SCLC cells and further induces a more invasive phenotype *in vitro*.

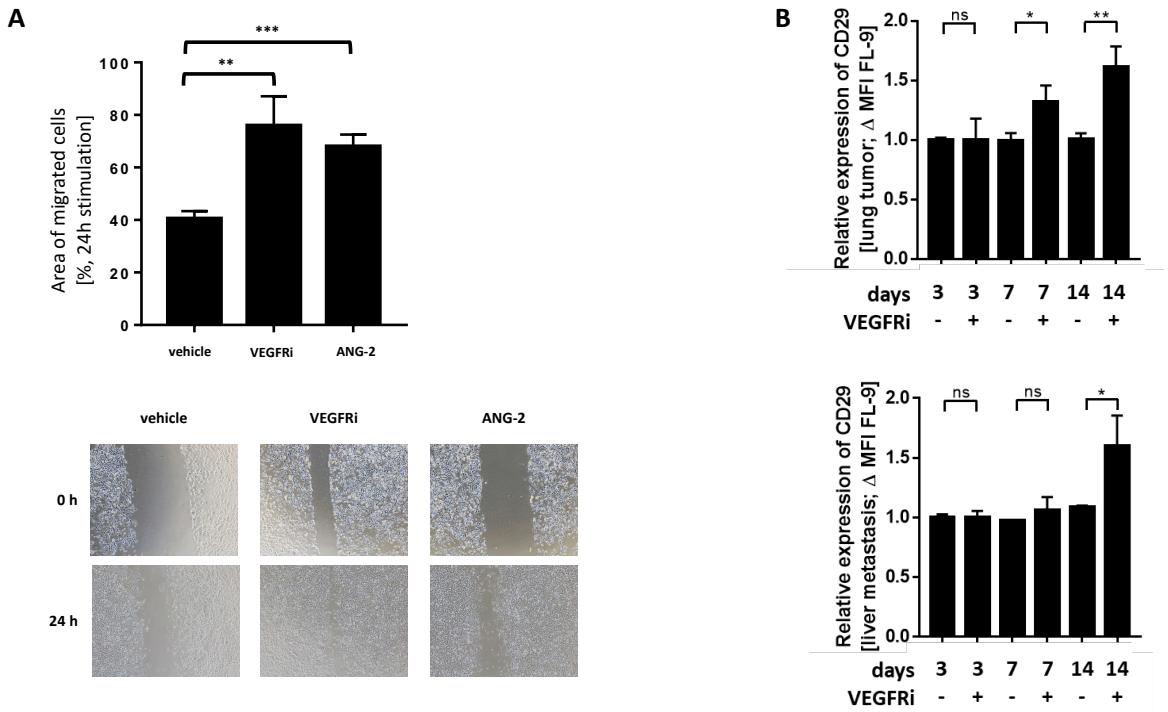

Figure 6: VEGFRi signaling directly regulates CD29 expression and induces more invasive phenotype in vitro.

A. Area of migrated tumor cells in wound healing assay. Tumor cells isolated from liver metastasis of SCLC bearing mice were treated with vehicle, VEGFR inhibitor Vatalanib (VEGFRi), or Angiopoietin-2 (ANG-2) for 24h. Representative images for each condition after 0h and 24h are shown.

B. Relative expression of CD29 on tumor cell lines in culture, isolated from primary lung tumor or from liver metastasis. Tumor cell lines were treated with VEGFR inhibitor Vatalanib (VEGFRi) or vehicle for 14 consecutive days. Flow cytometry was performed on days 3, 7 and 14. Relative expression is indicated as fold change, normalized to expression level of vehicle.

Statistical analysis was done using the Student's t-test (ns, not significant; *, $p < 0.05$; **, $p < 0,01$;***, $p < 0,001$; error bars, SEM). These experiments were conducted and analyzed by C. Otto. This figure contains unpublished data that is adapted from *"under revision".*

4.7 INCREASED LIVER METASTASIS FORMATION UPON VEGFR SIGNALING INHIBITION IS RESCUED BY ANTI-ANG2 TREATMENT *IN VIVO*

In concordance with our previously described *in vitro* results that show a more invasive phenotype upon VEGFRi treatment (Figure 6 A), we observed in *in vivo* experiments that VEGFRi monotherapy induced a significantly more extensive liver metastasis formation compared to control group treated tumor bearing mice (Figure 7). Furthermore, livers of mice treated with anti-ANG-2 antibody harbored a lower average count of metastatic tumor foci than of mice treated with vehicle and IgG control. The additional administration of anti-ANG-2 antibody to VEGFRi treatment could significantly suppress the pro-metastatic effect of VEGFRi monotherapy to a liver metastasis level below that of mice treated with vehicle and IgG control

(Figure 7). It can be concluded that an impairment of the VEGF-A/VEGFR signaling pathway leads to a significantly higher rate of liver metastasis. (*under revision*)

In summary, VEGFR signaling inhibition led to an increased formation of liver metastases, which was rescued *in vivo* by additional anti-ANG-2 treatment.

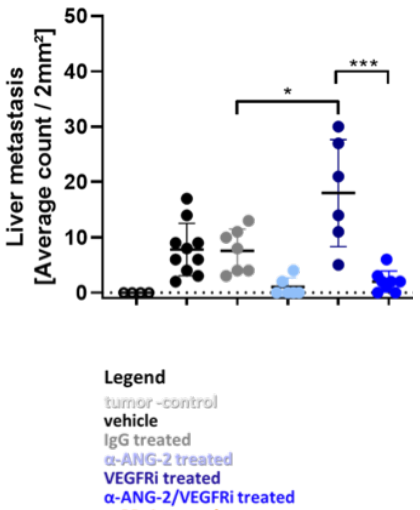

Figure 7: Increased liver metastasis formation upon blockade of VEGF signaling is rescued by anti-ANG2 treatment.

The liver metastasis screen was performed within the endpoint analysis and included macroscopical and microscopical screening of the liver for metastases. To quantify the liver metastasis formation, tumor cells were stained using CD56 antibody and the number of tumor cell foci (>10 cells) per 2mm^2 were counted.

SCLC-bearing mice were treated with vehicle control (vehicle; n=10), IgG control (IgG; *n* =7), anti-ANG-2 monotherapy (aANG-2; n=6), VEGFR inhibitor monotherapy (VEGFRi; *n* =6), and anti-ANG-2/VEGFRi combination therapy (aANG-2/VEGFRi; n=8). Upon detection of progressive disease based on µCT measurements and mouse adapted RECIST v1.1 criteria, endpoint analysis was performed and livers were screened for metastases. Tumor control was obtained from livers of mice without primary lung tumors.

Statistical analysis was done using the Student's t-test (ns, not significant; *, $p < 0.05$; **, $p < 0,01$;***, $p < 0,001$; error bars, SEM). The analysis was conducted by L. Meder. The experimental procedures and animal care were conducted by L. Meder, C. Otto and medical-technical assistant M. Nill. This figure contains unpublished data that is adapted from *under revision*.

4.8 RNA SEQUENCING REVEALED METASTASIS AND INVASION ASSOCIATED GENES THAT WERE UPREGULATED UPON VEGF-A-KNOCKOUT

Based on the VEGF-A/VEGFR signaling associated gain in invasive properties we performed mRNA sequencing to possibly identify tumor-cell associated signaling pathways which might be suitable targets for therapy upon progressive SCLC. We compared the genomic profile of 2 VEGF-A-knockout (KO) SCLC cell lines (VEGFA_KO_1 and VEGFA_KO_2) to the VEGF-

A wildtype empty vector SCLC cell line (empty vector). We found several genes that were up- or downregulated in the VEGF-A-KO SCLC cell lines compared to the VEGF-A wildtype (empty vector; eV) SCLC cell lines.

Gene symbol	Protein	UP/DOWN in VEGFAKO	log2fc (VEGFA_KO_1/empty vector)	log2fc (VEGFA_KO_2/empty vector)
Cdk6	Cyclin dependent kinase 6	UP	1,050004486	1,429647889
Cxcr4	C-X-C chemokine receptor type 4, CD184	UP	1,137393329	1,894264424
Eya2	Eyes absent homolog 2	UP	2,990448442	1,3007895
Fgf13	Fibroblast growth factor 13	UP	4,359553214	2,923272295
Id4	ID-4	UP	3,468849039	2,951796271
Mmp11	Metallo matrix proteinase 11	UP	1,633479634	1,40362199
Nedd9	Neural precursor cell expressed developmentally down-regulated protein 9	UP	1,670138498	1,371798663
Tnfsf12	Tumor necrosis factor ligand superfamily member 12	UP	1,089683128	1,236386933
Grhl2	Grainyhead-like protein 2 homolog	DOWN	-1,014865818	-1,650815255

Table 1. RNA Sequencing revealed metastasis and invasion associated genes that were upregulated upon VEGFA-Knockout.

RNA sequencing of VEGF-A knockout and VEGF-A wildtype empty vector SCLC cells was performed. To distinguish between UP/ DOWN in VEGF-A KO we used the following cut off:

- Log_2 fold change (VEGFA_KO_1/empty vector) >1 and log_2 fold change (VEGFA_KO_2/empty vector) >1 = UP
- Log_2 fold change (VEGFA_KO_1/empty vector) <1 and Log_2 fold change (VEGFA_KO_2/empty vector) <1 = DOWN

The preparation of the samples was conducted by C. Otto. The RNA-sequencing was conducted by the Cologne Center for Genomics (CCG) as core-facility in return for payment of a fee paid by the PI and supervisor of my thesis, Prof. Dr. Dr. Ullrich. The results were analyzed by C. Otto with the help of S. Borchmann.

The cut-off was a log_2(VEGF-A-KO/VEGF-A eV) >1/ <1, which is equivalent to a doubling/ halving of gene expression. To further narrow down the altered genes, we have selected the following genes (Table 1), of which a metastasis-relevant effect has been described in the literature [114-122].

In accordance to my study aims, I found an immunosupportive and tumor-suppressive role of targeting ANG-2 in SCLC treatment. Thereby, a combined therapeutic approach targeting

ANG-2, VEGFR and PD-1 significantly prolonged survival of mice and decreased liver metastasis formation. The metastatic phenotype of SCLC which was frequently observed upon VEGF-A/VEGFR signaling blockade, is likely driven by an ANG-2/CD29 dependent mechanism activating the intracellular kinases FAK and c-SRC.

5 DISCUSSION

5.1 RATIONALE TO COMBINE PD-1/ ANG-2/ VEGFR BLOCKADE TO TREAT SCLC

We showed that combined blockade of ANG-2, VEGFR and PD-1 significantly prolonged overall and progression-free survival of mice suffering from SCLC. Immunotherapy, for instance by blockade of PD-1, has emerged as novel therapeutic approach to attack malignant diseases. Over the years it has become apparent that also solid tumors can be efficiently targeted with immune checkpoint inhibitors [54]. In the year of 2018 the first line therapy for the treatment of SCLC was adapted by the inclusion of PD-L1 inhibitor Atezolizumab in addition to classical platinum-based chemotherapy, highlighting the rising relevance of immunotherapy in the treatment of lung cancer [35].

However, the development of resistances limits the antitumor effect of immunotherapy [55]. Furthermore, the highly dysfunctional tumor vasculature as well as direct immunosuppressive characteristics of the proangiogenic cytokines VEGF and ANG-2 are of major relevance for limited antitumoral effects of immunotherapy. In addition to its major role in angiogenesis, VEGF exerts various immunosuppressive effects in the tumor microenvironment [123]. VEGF-A produced by the tumor was shown to impair proliferation and effector functions of $CD8^+$ T-cells through upregulation of inhibitory immune checkpoints like PD-1, which was reverted by targeting the VEGF-A/VEGFR signaling axis [95]. In addition, high levels of VEGF-A are associated with diminished dendritic cell maturation and thus cause defects in antigen presentation [124]. Furthermore, VEGF-A can suppress T-cell development and promote the recruitment and proliferation of immunosuppressive regulatory T-cells, MDSCs and M2 polarized macrophages [91,125,126]. Analogously, ANG-2 exerts various immunosuppressive functions. Stimulation with ANG-2 *in vitro* augments expression of genes encoding for the potent immunosuppressive cytokine IL-10 and the T_{reg} attractant chemokine CCL17 in TIE2-expressing monocytes (TEMs). Through this mechanism ANG-2 is able to suppress T-cell proliferation and to promote expansion of the immunosuppressive T_{reg} population [127,128].

The immunosuppressive effects of both VEGF-A and ANG-2 that limit the effects of effective antitumor activity of PD-1 blockade based immunotherapy are in concordance with our results: We showed that the blockade of ANG-2 as well as VEGFR/VEGF-A signaling further improved the antitumor effect of PD-1 blockade in a synergistic manner. In line with our results, it was further shown that combined inhibition of PD-1, Angiopoietin-2 and VEGF improved survival in glioblastoma-bearing mice [129]. As we could not detect any direct effects of ANG-2 and/ or VEGF-A onto the T-cell activation status, we performed a cytokine array, analyzing the serum of mice treated with the different therapy regimens, in order to characterize the immunosupportive role of targeting ANG-2 and VEGF-A. Anti-ANG-2 monotherapy revealed the Custer A in our cytokine assay, that consists of IFN-g, IL-2, IL-9 and MIP-1a. A central characteristic of these cytokines is their association with the M1 polarized macrophages, that

exert proinflammatory and thus antitumoral effects [130-133]. The Cluster B, which consists of the cytokines IL-7 and IL-15, is altered upon anti-PD-1 monotherapy. IL-7 and IL-15 are known to also be proinflammatory and to support antitumor effects of the immune system by activating $CD8^+$ T-cells and antagonizing immunosuppressive networks [134,135]. Cluster C is referred to the triple combination therapy targeting ANG-2, VEGFR, and PD-1. It consists of IL-12, IL-1a, M-CSF and MIP-2; these cytokines are associated with an ambivalent immunogenic profile: Both IL-12 and IL-1a show proinflammatory characteristics and are affiliated with antitumoral M1 macrophage signature [130]. However, M-CSF is a potent inducer of M2 macrophage polarization, that is described to support tumor growth [136,137] and MIP-2 is characterized as a tumor supporting cytokine [138]. This might be reasoned by the fact that the serum samples have been harvested upon progressive disease status. However, M-CSF and MIP-2 show proangiogenic effects and we hypothesize that these cytokines may counteract the antiangiogenic therapy regimens and provide features of resistance [139,140]. Thus, this cytokine signature, which is ambivalent with respect to angiogenesis and immunosuppression, could be a potential trigger for disease progression in triple combination.

Taken together, we could confirm the rationale to combine PD-1/ ANG-2/ VEGFR blockade for the treatment of SCLC, as this combination therapy significantly increased the overall and progression-free survival of SCLC-bearing mice. Thereby, the anti-tumor activity of anti-PD-1 specific immunotherapy was enhanced by specific blockade of immunosuppressive VEGF-A/VEGFR -signaling axis and ANG-2.

5.2 ANG-2/ CD29 SIGNALING TRIGGERS SCLC METASTASIS FORMATION

Flow cytometry-based characterization of the murine tumor cell lines, isolated from primary lung tumors as well as from liver metastases revealed that the main ANG-2 receptor TIE-2 was not expressed. Instead various integrins including CD61, CD49 and CD29 were highly expressed. In concordance with our result, Felcht *et al.* analogously described a subpopulation of TIE-2 negative endothelial cells that were in turn characterized by abundant expression of integrins [141].

Besides to the TIE-2 receptor, ANG-2 can bind to integrins, which describe a family of 24 heterodimers, generated by a combination of alpha and beta subunits. Integrins are the main cellular adhesion receptors through mediation of cell-cell and cell-ECM (extracellular matrix) interactions and they are therefore ubiquitously expressed on several cell types including immune cells, ECs, fibroblasts and tumor cells. The ligands are diverse with a focus on components of the ECM but also ANG-2 is capable of integrin activation. Upon activation, integrins may regulate intercellular integrity, cell motility, and invasion [142,143]. In general, given the central role of integrins in cellular adhesion, mechanotransduction, cell motility and migration, they are involved in nearly every step of cancer progression [143]. Integrins contribute

to the primary tumor initiation and may promote migration and invasiveness in a later stage. Integrin activity is further highly relevant in the formation of premetastatic niches and the tumor cells' extravasation from the capillary to the adjacent tissue that is to be colonized, demonstrating their significance in metastatic cancer progression [143]. Hakanpaa *et al.* reported as well, that in TIE-2 deficient endothelial cells ANG-2 is able to maintain the actin cytoskeleton structure via integrin-β1 activation towards a destabilized endothelium that facilitates tumor cell migration, which highlights the role of CD29 in invasiveness of tumor cells [110].

Binding of the ligand, for example ANG-2, to integrin-β1 results in internalization of the integrin followed by autophosphorylation and activation of the integrin adaptor protein Focal adhesion Kinase (FAK) [111]. The phosphorylated state of FAK allows proteins, containing the SH2 domain to bind to FAK, which further potentiates the activity of FAK. C-SRC kinase, which features the SH2 domain, can bind to FAK and is activated through this mechanism [144]. In accordance to this pathway we showed in our western blot analysis that stimulation of murine SCLC cells with ANG-2 led to the activating phosphorylation of FAK at Y397 and of c-SRC at Y416. The activated FAK (Y397) and c-SRC (Y416) kinases are reported to promote invasive and angiogenic properties of the activated cells [141,145,146]. Also Zhao *et al.* described that stabilization of integrin-β1 leads to an increased activation of FAK and c-SRC kinase that in turn promotes SCLC metastasis formation and should be therefore considered as a therapeutic target [147]. In a retrospective analysis of FFPE tissue from lung cancer patients it was shown that expression levels of activated FAK were significantly higher in lung cancer tissue than in non-tumor lung tissue and significantly higher in SCLC than in NSCLC [148]. Besides its major role as a regulator of cell motility and migration, FAK is a potent stimulator of tumor immune evasion. Its kinase activity promotes exhaustion of $CD8^+$ T-cells and recruits regulatory T-cells to the TME [149]. Further, targeting FAK with FAK inhibitor VS-4718 rendered previously unresponsive pancreatic tumors sensitive to anti-CTLA4 / anti-PD-1 immunotherapy by decreasing immunosuppressive cell populations in the TME in mouse model of pancreatic ductal adenocarcinoma [150].

Demonstrating the prominent role of integrin-β1 in ANG-2 promoted invasiveness, breast cancer cells were shown to gain metastatic properties through integrin-β1 mediated ANG-2 stimulation that led to epithelial-mesenchymal transition (EMT) [111,151]. It was further evaluated that β1-integrins are essential for the transendothelial invasion of the tumor cells into the adjacent tissue past the basal membrane [152]. And in particular for SCLC, the role of CD29 as a prognostic marker has been described several times [153,154]. Based on these results we evaluated the expression levels of CD29 on tumor cells using flow cytometry: it revealed significantly higher expression levels of CD29 on tumor cells that were isolated from primary lung tumors of mice with visible liver metastases than of mice without visible liver metastases. The CD29 expression levels were even higher on tumor cells, isolated directly from liver

metastases, which is in accordance with the above-mentioned integrin-mediated invasive characteristics.

In summary, we showed that the binding of ANG-2 to its ligand integrin-β1, which was elevated upon metastasis formation, leads to activating phosphorylation of FAK and c-SRC and may trigger metastasis via this signaling pathway.

5.3 VEGFR INHIBITION DIRECTLY REGULATES CD29 EXPRESSION AND SCLC METASTASIS

We further showed that *in vitro* stimulation of tumor cells with VEGFR inhibitor "Vatalanib" for 14 consecutive days led to a significant steady increase of CD29 expression level, highlighting the potential role of CD29 as a mediator in VEGFRi induced gain of invasive properties. In coherence with our hypothesis, we were able to show increased migratory capabilities of tumor cells upon treatment with the VEGFR inhibitor in wound healing assays. Similar results were obtained upon ANG-2 stimulation. As both stimulation with CD29 ligand as well as stimulation with CD29 inducer promote the invasive phenotype, these results highlight the role of CD29 in ANG-2 and VEGF-A signaling associated promotion of invasiveness.

Following our *in vitro* results, we showed *in vivo* that mice treated with VEGFR inhibitor harbored a significantly increased number of liver metastasis foci compared to control mice. In concordance with our results Volz *et al.* showed that the inhibition of tumor VEGFR2 induced tumor cell invasion and metastasis formation in Non-small cell lung cancer [100]. Also in other tumor entities therapeutic blockade of VEGF signaling pathway was shown to trigger a more invasive phenotype [155,156].

In order to obtain clearer insight into the potential mechanisms leading to the more invasive phenotype as a result of blockade of the VEGF signaling pathway, we performed mRNA sequencing, using VEGF-A knockout (KO) vs empty vector (eV) control cell lines. The mRNA sequencing revealed several genes, that were up- or downregulated in the VEGF-A KO compared to our eV control. In the analysis of these results we focused on genes, that were described in literature to have a metastatic-relevant effect [114-122]. Among other genes we found *Nedd9* to be higher expressed in VEGFA-KO cells. NEDD9 (Neural precursor cell-expressed developmentally downregulated 9) overexpression was found to be associated to metastasis promotion in various human solid tumors [118,157,158]. In this context, Sima *et al.* assign an important role to the phosphorylation of FAK and SRC [159]. Further, we found higher expression levels of *Cdk6* in VEGF-A KO cells, which is described to be relevant in the formation of metastasis [160,161]. A clinical phase 2 trial, targeting CDK6 in chemotherapy refractory extensive stage SCLC is ongoing (NCT04010357, status "recruiting" in January 2023) and the role of CDK6 inhibition might be investigated in follow-up projects to overcome SCLC metastasis.

We were moreover successful to demonstrate that in turn therapeutic ANG-2 blockade led to a decreased level of liver metastasis formation that was even lower than that of the IgG treated mice. The additional antibody-mediated blockade of ANG-2 abrogated the increased metastasis formation induced by VEGFR inhibition. This anti-metastatic effect of ANG-2 blockade is in accordance with Holopainen *et al.* who reported enhanced endothelial cell integrity upon ANG-2 blockade that thereby inhibited metastatic dissemination [103].

These preclinical findings emphasize the role of ANG-2 in metastasis formation and as a potential anti-angiogenesis target suitable for implementation in combined therapy approaches in the clinic.

CONCLUSION

Concluding, we demonstrated that targeting of ANG-2 and VEGF-A has an immunosupportive effect and hence, when combined with PD-1 blockade-based immunotherapy, the survival of SCLC-bearing mice was significantly prolonged. Moreover, we showed that VEGFR inhibitor therapy induced increased SCLC invasiveness, both *in vivo* and *in vitro*, with integrin-β1 playing a central role. The additional antagonization of ANG-2, the ligand for integrin-β1, in turn significantly suppressed liver metastasis formation.

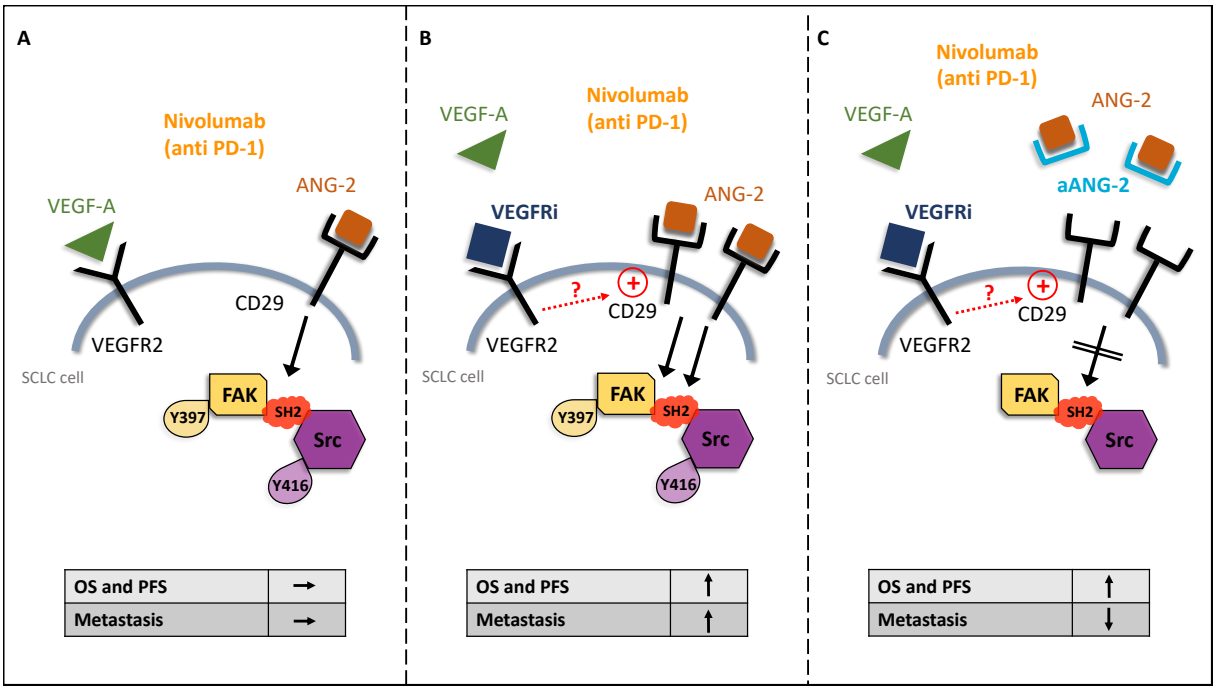

Figure 8: Graphical Abstract.

A. SCLC cells express VEGFR2 and CD29 on their surface. Upon binding of CD29 ligand ANG-2, FAK and SRC kinase are activated by phosphorylation (FAK: Y397; SRC: Y416) and metastasis is on a base level. Nivolumab treatment results in a base level of OS and PFS.

B. Upon blockade of VEGFR with VEGFRi, CD29 expression level on SCLC cells is enhanced. Thus, downstream activation of FAK and SRC is enhanced and metastasis is promoted. Combined treatment of VEGFRi and Nivolumab leads to increased OS and PFS compared to Nivolumab monotherapy.

C. Blockade of ANG-2 may interrupt FAK and SRC phosphorylation and therefore, metastasis can be suppressed. Triple combination treatment with Nivolumab, VEGFRi, and anti-ANG-2 leads to increased OS and PFS compared to Nivolumab monotherapy.

This figure was designed by C. Otto and is adapted from *"under revision"*.

Since the combined therapy of VEGFR, ANG-2 and PD-1 blockade prolonged survival and reduced the metastasis rate, we suggest based on these preclinical results, to implement this therapy in the clinic as it is anticipated to provide a direct benefit to patients suffering from SCLC.

6 LITERATURE

1. Country statistics and global health estimates by WHO and UN partners of the year 2015. 2015. https://www.who.int/gho/countries/deu.pdf?ua=1 (Last consulted online on March 27th, 2020).

2. Bericht zum Krebsgeschehen in Deutschland 2016. Zentrum für Krebsregisterdaten im Robert Koch-Institut. 2016. https://www.krebsdaten.de/Krebs/DE/Content/Publikationen/Krebs_in_Deutschland/kid_2019/krebs_in_deutschland_2019.pdf?__blob=publicationFile (Last consulted online on February 4th, 2020).

3. Clinical Lung Cancer Genome P, Network Genomic M. A genomics-based classification of human lung tumors. *Sci Transl Med* 2013; **5**(209): 209ra153.

4. Karachaliou N, Pilotto S, Lazzari C, Bria E, de Marinis F, Rosell R. Cellular and molecular biology of small cell lung cancer: an overview. *Transl Lung Cancer Res* 2016; **5**(1): 2-15.

5. Govindan R, Page N, Morgensztern D, et al. Changing epidemiology of small-cell lung cancer in the United States over the last 30 years: analysis of the surveillance, epidemiologic, and end results database. *J Clin Oncol* 2006; **24**(28): 4539-44.

6. van Meerbeeck JP, Fennell DA, De Ruysscher DK. Small-cell lung cancer. *Lancet* 2011; **378**(9804): 1741-55.

7. Gandhi L, Johnson BE. Paraneoplastic syndromes associated with small cell lung cancer. *J Natl Compr Canc Netw* 2006; **4**(6): 631-8.

8. Pelosof LC, Gerber DE. Paraneoplastic syndromes: an approach to diagnosis and treatment. *Mayo Clin Proc* 2010; **85**(9): 838-54.

9. Chute JP, Taylor E, Williams J, Kaye F, Venzon D, Johnson BE. A metabolic study of patients with lung cancer and hyponatremia of malignancy. *Clin Cancer Res* 2006; **12**(3 Pt 1): 888-96.

10. Terzolo M, Reimondo G, Ali A, et al. Ectopic ACTH syndrome: molecular bases and clinical heterogeneity. *Ann Oncol* 2001; **12 Suppl 2**: S83-7.

11. Payne M, Bradbury P, Lang B, et al. Prospective study into the incidence of Lambert Eaton myasthenic syndrome in small cell lung cancer. *J Thorac Oncol* 2010; **5**(1): 34-8.

12. Argiris A, Murren JR. Staging and clinical prognostic factors for small-cell lung cancer. *Cancer J* 2001; **7**(5): 437-47.

13. Gaspar LE, McNamara EJ, Gay EG, et al. Small-cell lung cancer: prognostic factors and changing treatment over 15 years. *Clin Lung Cancer* 2012; **13**(2): 115-22.

14. Travis WD. Pathology and diagnosis of neuroendocrine tumors: lung neuroendocrine. *Thorac Surg Clin* 2014; **24**(3): 257-66.

15. Thomas A, Pommier Y. Small cell lung cancer: Time to revisit DNA-damaging chemotherapy. *Sci Transl Med* 2016; **8**(346): 346fs12.

16. Pietanza MC, Ladanyi M. Bringing the genomic landscape of small-cell lung cancer into focus. *Nat Genet* 2012; **44**(10): 1074-5.

17. George J, Lim JS, Jang SJ, et al. Comprehensive genomic profiles of small cell lung cancer. *Nature* 2015; **524**(7563): 47-53.

18. Hinds PW, Weinberg RA. Tumor-Suppressor Genes. *Curr Opin Genet Dev* 1994; **4**(1): 135-41.

19. Peifer M, Fernandez-Cuesta L, Sos ML, et al. Integrative genome analyses identify key somatic driver mutations of small-cell lung cancer. *Nat Genet* 2012; **44**(10): 1104-10.

20. Meder L, Buttner R, Odenthal M. Notch signaling triggers the tumor heterogeneity of small cell lung cancer. *J Thorac Dis* 2017; **9**(12): 4884-8.

21. Sutherland KD, Proost N, Brouns I, Adriaensen D, Song JY, Berns A. Cell of Origin of Small Cell Lung Cancer: Inactivation of Trp53 and Rb1 in Distinct Cell Types of Adult Mouse Lung. *Cancer Cell* 2011; **19**(6): 754-64.

22. Osada H, Tomida S, Yatabe Y, et al. Roles of achaete-scute homologue 1 in DKK1 and E-cadherin repression and neuroendocrine differentiation in lung cancer. *Cancer Res* 2008; **68**(6): 1647-55.

23. Meder L, Konig K, Ozretic L, et al. NOTCH, ASCL1, p53 and RB alterations define an alternative pathway driving neuroendocrine and small cell lung carcinomas. *Int J Cancer* 2016; **138**(4): 927-38.

24. Jiang TY, Collins BJ, Jin N, et al. Achaete-Scute Complex Homologue 1 Regulates Tumor-Initiating Capacity in Human Small Cell Lung Cancer. *Cancer Res* 2009; **69**(3): 845-54.

25. Lim JS, Ibaseta A, Fischer MM, et al. Intratumoural heterogeneity generated by Notch signalling promotes small-cell lung cancer. *Nature* 2017; **545**(7654): 360-4.

26. Saunders LR, Bankovich AJ, Anderson WC, et al. A DLL3-targeted antibody-drug conjugate eradicates high-grade pulmonary neuroendocrine tumor-initiating cells in vivo. *Sci Transl Med* 2015; **7**(302): 302ra136.

27. Sabari JK, Lok BH, Laird JH, Poirier JT, Rudin CM. Unravelling the biology of SCLC: implications for therapy. *Nature Reviews Clinical Oncology* 2017; **14**(9): 549-61.

28. Scheel AH, Dietel M, Heukamp LC, et al. Harmonized PD-L1 immunohistochemistry for pulmonary squamous-cell and adenocarcinomas. *Mod Pathol* 2016; **29**(10): 1165-72.

29. Scheel AH, Dietel M, Heukamp LC, et al. [Predictive PD-L1 immunohistochemistry for non-small cell lung cancer : Current state of the art and experiences of the first German harmonization study]. *Pathologe* 2016; **37**(6): 557-67.

30. Schultheis AM, Scheel AH, Ozretic L, et al. PD-L1 expression in small cell neuroendocrine carcinomas. *Eur J Cancer* 2015; **51**(3): 421-6.

31. Carvajal-Hausdorf D, Altan M, Velcheti V, et al. Expression and clinical significance of PD-L1, B7-H3, B7-H4 and TILs in human small cell lung Cancer (SCLC). *J Immunother Cancer* 2019; **7**(1): 65.

32. Tsuruoka K, Horinouchi H, Goto Y, et al. PD-L1 expression in neuroendocrine tumors of the lung. *Lung Cancer* 2017; **108**: 115-20.

33. Wang H, Li Z, Dong B, et al. Prognostic significance of PD-L1 expression and CD8+ T cell infiltration in pulmonary neuroendocrine tumors. *Diagn Pathol* 2018; **13**(1): 30.

34. Leitlinienprogramm Onkologie (Deutsche Krebsgesellschaft, Deutsche Krebshilfe, AWMF): Prävention, Diagnostik, Therapie und Nachsorge des Lungenkarzinoms. 2018. http://leitlinienprogramm-onkologie.de/Lungenkarzinom.98.0.html (Last consulted online on March 10th, 2020).

35. Horn L, Mansfield AS, Szczesna A, et al. First-Line Atezolizumab plus Chemotherapy in Extensive-Stage Small-Cell Lung Cancer. *N Engl J Med* 2018; **379**(23): 2220-9.

36. Ariyan CE, Brady MS, Siegelbaum RH, et al. Robust Antitumor Responses Result from Local Chemotherapy and CTLA-4 Blockade. *Cancer Immunol Res* 2018; **6**(2): 189-200.

37. Hui R, Garon EB, Goldman JW, et al. Pembrolizumab as first-line therapy for patients with PD-L1-positive advanced non-small cell lung cancer: a phase 1 trial. *Ann Oncol* 2017; **28**(4): 874-81.

38. Nanda R, Chow LQM, Dees EC, et al. Pembrolizumab in Patients With Advanced Triple-Negative Breast Cancer: Phase Ib KEYNOTE-012 Study. *J Clin Oncol* 2016; **34**(21): 2460-+.

39. Chen DS, Mellman I. Oncology meets immunology: the cancer-immunity cycle. *Immunity* 2013; **39**(1): 1-10.

40. Conway JR, Kofman E, Mo SS, Elmarakeby H, Van Allen E. Genomics of response to immune checkpoint therapies for cancer: implications for precision medicine. *Genome Med* 2018; **10**(1): 93.

41. Collins AV, Brodie DW, Gilbert RJC, et al. The interaction properties of costimulatory molecules revisited. *Immunity* 2002; **17**(2): 201-10.

42. Zou WP, Wolchok JD, Chen LP. PD-L1 (B7-H1) and PD-1 pathway blockade for cancer therapy: Mechanisms, response biomarkers, and combinations. *Sci Transl Med* 2016; **8**(328).

43. Dong HD, Strome SE, Salomao DR, et al. Tumor-associated B7-H1 promotes T-cell apoptosis: A potential mechanism of immune evasion. *Nat Med* 2002; **8**(8): 793-800.

44. Pardoll DM. The blockade of immune checkpoints in cancer immunotherapy. *Nature Reviews Cancer* 2012; **12**(4): 252-64.

45. Reck M, Heigener D, Reinmuth N. Immunotherapy for small-cell lung cancer: emerging evidence. *Future Oncology* 2016; **12**(7): 931-43.

46. Iwai Y, Ishida M, Tanaka Y, Okazaki T, Honjo T, Minato N. Involvement of PD-L1 on tumor cells in the escape from host immune system and tumor immunotherapy by PD-L1 blockade. *Proc Natl Acad Sci U S A* 2002; **99**(19): 12293-7.

47. Parsa AT, Waldron JS, Panner A, et al. Loss of tumor suppressor PTEN function increases B7-H1 expression and immunoresistance in glioma. *Nat Med* 2007; **13**(1): 84-8.

48. Zhao JF, Chen AX, Gartrell RD, et al. Immune and genomic correlates of response to anti-PD-1 immunotherapy in glioblastoma (vol 25, pg 462, 2019). *Nat Med* 2019; **25**(6): 1022-.

49. Marzec M, Zhang Q, Goradia A, et al. Oncogenic kinase NPM/ALK induces through STAT3 expression of immunosuppressive protein CD274 (PD-L1, B7-H1). *Proc Natl Acad Sci U S A* 2008; **105**(52): 20852-7.

50. Ivashkiv LB. IFN gamma: signalling, epigenetics and roles in immunity, metabolism, disease and cancer immunotherapy. *Nature Reviews Immunology* 2018; **18**(9): 545-58.

51. Chen S, Crabill GA, Pritchard TS, et al. Mechanisms regulating PD-L1 expression on tumor and immune cells. *J Immunother Cancer* 2019; **7**(1): 305.

52. Miller JFAP, Sadelain M. The Journey from Discoveries in Fundamental Immunology to Cancer Immunotherapy. *Cancer Cell* 2015; **27**(4): 439-49.

53. Wang Y, Wu L, Tian C, Zhang YZ. PD-1-PD-L1 immune-checkpoint blockade in malignant lymphomas. *Ann Hematol* 2018; **97**(2): 229-37.

54. Kruger S, Ilmer M, Kobold S, et al. Advances in cancer immunotherapy 2019-latest trends. *J Exp Clin Cancer Res* 2019; **38**.

55. Sharma P, Hu-Lieskovan S, Wargo JA, Ribas A. Primary, Adaptive, and Acquired Resistance to Cancer Immunotherapy. *Cell* 2017; **168**(4): 707-23.

56. van Rooij N, van Buuren MM, Philips D, et al. Tumor Exome Analysis Reveals Neoantigen-Specific T-Cell Reactivity in an Ipilimumab-Responsive Melanoma. *J Clin Oncol* 2013; **31**(32): E439-E42.

57. Gubin MM, Zhang XL, Schuster H, et al. Checkpoint blockade cancer immunotherapy targets tumour-specific mutant antigens. *Nature* 2014; **515**(7528): 577-+.

58. Sucker A, Zhao F, Real B, et al. Genetic Evolution of T-cell Resistance in the Course of Melanoma Progression. *Clin Cancer Res* 2014; **20**(24): 6593-604.

59. Benci JL, Xu BH, Qiu Y, et al. Tumor Interferon Signaling Regulates a Multigenic Resistance Program to Immune Checkpoint Blockade. *Cell* 2016; **167**(6): 1540-+.

60. Ebert PJR, Cheung J, Yang YG, et al. MAP Kinase Inhibition Promotes T Cell and Anti-tumor Activity in Combination with PD-L1 Checkpoint Blockade. *Immunity* 2016; **44**(3): 609-21.

61. Garrido F, Aptsiauri N, Doorduijn EM, Garcia Lora AM, van Hall T. The urgent need to recover MHC class I in cancers for effective immunotherapy. *Curr Opin Immunol* 2016; **39**: 44-51.

62. Sade-Feldman M, Jiao YJ, Chen JH, et al. Resistance to checkpoint blockade therapy through inactivation of antigen presentation. *Nat Commun* 2017; **8**(1): 1136.

63. Zaretsky JM, Garcia-Diaz A, Shin DS, et al. Mutations Associated with Acquired Resistance to PD-1 Blockade in Melanoma. *N Engl J Med* 2016; **375**(9): 819-29.

64. Alexandrov LB, Nik-Zainal S, Wedge DC, et al. Signatures of mutational processes in human cancer (vol 500, pg 415, 2013). *Nature* 2013; **502**(7470).

65. Rizvi NA, Hellmann MD, Snyder A, et al. Cancer immunology. Mutational landscape determines sensitivity to PD-1 blockade in non-small cell lung cancer. *Science* 2015; **348**(6230): 124-8.

66. Hellmann MD, Callahan MK, Awad MM, et al. Tumor Mutational Burden and Efficacy of Nivolumab Monotherapy and in Combination with Ipilimumab in Small-Cell Lung Cancer. *Cancer Cell* 2019; **35**(2): 329.

67. Calles A, Aguado G, Sandoval C, Alvarez R. The role of immunotherapy in small cell lung cancer. *Clin Transl Oncol* 2019; **21**(8): 961-76.

68. Doyle A, Martin WJ, Funa K, et al. Markedly decreased expression of class I histocompatibility antigens, protein, and mRNA in human small-cell lung cancer. *J Exp Med* 1985; **161**(5): 1135-51.

69. Yu H, Batenchuk C, Badzio A, et al. PD-L1 Expression by Two Complementary Diagnostic Assays and mRNA In Situ Hybridization in Small Cell Lung Cancer. *J Thorac Oncol* 2017; **12**(1): 110-20.

70. Antonia SJ, Lopez-Martin JA, Bendell J, et al. Nivolumab alone and nivolumab plus ipilimumab in recurrent small-cell lung cancer (CheckMate 032): a multicentre, open-label, phase 1/2 trial. *Lancet Oncol* 2016; **17**(7): 883-95.

71. Iams WT, Porter J, Horn L. Immunotherapeutic approaches for small-cell lung cancer. *Nat Rev Clin Oncol* 2020; **17**(5): 300-12.

72. Huang YH, Kim BYS, Chan CK, Hahn SM, Weissman IL, Jiang W. Improving immune-vascular crosstalk for cancer immunotherapy. *Nature Reviews Immunology* 2018; **18**(3): 195-203.

73. Schaaf MB, Garg AD, Agostinis P. Defining the role of the tumor vasculature in antitumor immunity and immunotherapy. *Cell Death Dis* 2018; **9**(2): 115.

74. Hanahan D, Weinberg RA. Hallmarks of Cancer: The Next Generation. *Cell* 2011; **144**(5): 646-74.

75. Potente M, Gerhardt H, Carmeliet P. Basic and therapeutic aspects of angiogenesis. *Cell* 2011; **146**(6): 873-87.

76. Bergers G, Benjamin LE. Tumorigenesis and the angiogenic switch. *Nat Rev Cancer* 2003; **3**(6): 401-10.

77. Vaupel P, Mayer A. Hypoxia in cancer: significance and impact on clinical outcome. *Cancer Metastasis Rev* 2007; **26**(2): 225-39.

78. LaGory EL, Giaccia AJ. The ever-expanding role of HIF in tumour and stromal biology. *Nat Cell Biol* 2016; **18**(4): 356-65.

79. Phng LK, Gerhardt H. Angiogenesis: a team effort coordinated by notch. *Dev Cell* 2009; **16**(2): 196-208.

80. De Palma M, Biziato D, Petrova TV. Microenvironmental regulation of tumour angiogenesis. *Nat Rev Cancer* 2017; **17**(8): 457-74.

81. Baluk P, Morikawa S, Haskell A, Mancuso M, McDonald DM. Abnormalities of basement membrane on blood vessels and endothelial sprouts in tumors. *Am J Pathol* 2003; **163**(5): 1801-15.

82. Lewis JS, Landers RJ, Underwood JCE, Harris AL, Lewis CE. Expression of vascular endothelial growth factor by macrophages is up-regulated in poorly vascularized areas of breast carcinomas. *J Pathol* 2000; **192**(2): 150-8.

83. Harney AS, Arwert EN, Entenberg D, et al. Real-Time Imaging Reveals Local, Transient Vascular Permeability, and Tumor Cell Intravasation Stimulated by TIE2hi Macrophage-Derived VEGFA. *Cancer Discov* 2015; **5**(9): 932-43.

84. Leek RD, Lewis CE, Whitehouse R, Greenall M, Clarke J, Harris AL. Association of macrophage infiltration with angiogenesis and prognosis in invasive breast carcinoma. *Cancer Res* 1996; **56**(20): 4625-9.

85. Clear AJ, Lee AM, Calaminici M, et al. Increased angiogenic sprouting in poor prognosis FL is associated with elevated numbers of CD163(+) macrophages within the immediate sprouting microenvironment. *Blood* 2010; **115**(24): 5053-6.

86. Liang W, Ferrara N. The Complex Role of Neutrophils in Tumor Angiogenesis and Metastasis. *Cancer Immunol Res* 2016; **4**(2): 83-91.

87. Muller WA. Mechanisms of Leukocyte Transendothelial Migration. *Annu Rev Pathol-Mech* 2011; **6**: 323-44.

88. Bouzin C, Brouet A, De Vriese J, DeWever J, Feron O. Effects of vascular endothelial growth factor on the lymphocyte-endothelium interactions: Identification of caveolin-1 and nitric oxide as control points of endothelial cell anergy. *J Immunol* 2007; **178**(3): 1505-11.

89. Dirkx AE, Oude Egbrink MG, Kuijpers MJ, et al. Tumor angiogenesis modulates leukocyte-vessel wall interactions in vivo by reducing endothelial adhesion molecule expression. *Cancer Res* 2003; **63**(9): 2322-9.

90. Wu XQ, Giobbie-Hurder A, Liao XY, et al. VEGF Neutralization Plus CTLA-4 Blockade Alters Soluble and Cellular Factors Associated with Enhancing Lymphocyte Infiltration and Humoral Recognition in Melanoma. *Cancer Immunol Res* 2016; **4**(10): 858-68.

91. Fukurnura D, Kloepper J, Amoozgar Z, Duda DG, Jain RK. Enhancing cancer immunotherapy using antiangiogenics: opportunities and challenges. *Nature Reviews Clinical Oncology* 2018; **15**(5): 325-40.

92. Liu C, Peng W, Xu C, et al. BRAF inhibition increases tumor infiltration by T cells and enhances the antitumor activity of adoptive immunotherapy in mice. *Clin Cancer Res* 2013; **19**(2): 393-403.

93. Wu XQ, Giobbie-Hurder A, Liao XY, et al. Angiopoietin-2 as a Biomarker and Target for Immune Checkpoint Therapy. *Cancer Immunol Res* 2017; **5**(1): 17-28.

94. Schmittnaegel M, Rigamonti N, Kadioglu E, et al. Dual angiopoietin-2 and VEGFA inhibition elicits antitumor immunity that is enhanced by PD-1 checkpoint blockade. *Sci Transl Med* 2017; **9**(385).

95. Voron T, Colussi O, Marcheteau E, et al. VEGF-A modulates expression of inhibitory checkpoints on CD8+ T cells in tumors. *J Exp Med* 2015; **212**(2): 139-48.

96. Meder L, Schuldt P, Thelen M, et al. Combined VEGF and PD-L1 Blockade Displays Synergistic Treatment Effects in an Autochthonous Mouse Model of Small Cell Lung Cancer. *Cancer Res* 2018; **78**(15): 4270-81.

97. Yasuda S, Sho M, Yamato I, et al. Simultaneous blockade of programmed death 1 and vascular endothelial growth factor receptor 2 (VEGFR2) induces synergistic anti-tumour effect in vivo. *Clin Exp Immunol* 2013; **172**(3): 500-6.

98. Allen E, Jabouille A, Rivera LB, et al. Combined antiangiogenic and anti-PD-L1 therapy stimulates tumor immunity through HEV formation. *Sci Transl Med* 2017; **9**(385).

99. Wu FT, Man S, Xu P, et al. Efficacy of Cotargeting Angiopoietin-2 and the VEGF Pathway in the Adjuvant Postsurgical Setting for Early Breast, Colorectal, and Renal Cancers. *Cancer Res* 2016; **76**(23): 6988-7000.

100. Volz C, Breid S, Selenz C, et al. Inhibition of Tumor VEGFR2 Induces Serine 897 EphA2-Dependent Tumor Cell Invasion and Metastasis in NSCLC. *Cell Rep* 2020; **31**(4): 107568.

101. Mazzieri R, Pucci F, Moi D, et al. Targeting the ANG2/TIE2 axis inhibits tumor growth and metastasis by impairing angiogenesis and disabling rebounds of proangiogenic myeloid cells. *Cancer Cell* 2011; **19**(4): 512-26.

102. Srivastava K, Hu J, Korn C, et al. Postsurgical adjuvant tumor therapy by combining anti-angiopoietin-2 and metronomic chemotherapy limits metastatic growth. *Cancer Cell* 2014; **26**(6): 880-95.

103. Holopainen T, Saharinen P, D'Amico G, et al. Effects of angiopoietin-2-blocking antibody on endothelial cell-cell junctions and lung metastasis. *J Natl Cancer Inst* 2012; **104**(6): 461-75.

104. Gengenbacher N, Singhal M, Mogler C, et al. Timed Ang2-Targeted Therapy Identifies the Angiopoietin-Tie Pathway as Key Regulator of Fatal Lymphogenous Metastasis. *Cancer Discov* 2021; **11**(2): 424-45.

105. Morpheus, https://software.broadinstitute.org/morpheus (used in 2019 and 2020).

106. Meuwissen R, Linn SC, Linnoila RI, Zevenhoven J, Mooi WJ, Berns A. Induction of small cell lung cancer by somatic inactivation of both Trp53 and Rb1 in a conditional mouse model. *Cancer Cell* 2003; **4**(3): 181-9.

107. DuPage M, Dooley AL, Jacks T. Conditional mouse lung cancer models using adenoviral or lentiviral delivery of Cre recombinase. *Nat Protoc* 2009; **4**(7): 1064-72.

108. Eisenhauer EA, Therasse P, Bogaerts J, et al. New response evaluation criteria in solid tumours: revised RECIST guideline (version 1.1). *Eur J Cancer* 2009; **45**(2): 228-47.

109. Agata Y, Kawasaki A, Nishimura H, et al. Expression of the PD-1 antigen on the surface of stimulated mouse T and B lymphocytes. *Int Immunol* 1996; **8**(5): 765-72.

110. Hakanpaa L, Sipila T, Leppanen VM, et al. Endothelial destabilization by angiopoietin-2 via integrin beta1 activation. *Nat Commun* 2015; **6**: 5962.

111. Imanishi Y, Hu B, Jarzynka MJ, et al. Angiopoietin-2 stimulates breast cancer metastasis through the alpha(5)beta(1) integrin-mediated pathway. *Cancer Res* 2007; **67**(9): 4254-63.

112. Michael KE, Dumbauld DW, Burns KL, Hanks SK, Garcia AJ. Focal adhesion kinase modulates cell adhesion strengthening via integrin activation. *Mol Biol Cell* 2009; **20**(9): 2508-19.

113. Irtegun S, Wood RJ, Ormsby AR, Mulhern TD, Hatters DM. Tyrosine 416 is phosphorylated in the closed, repressed conformation of c-Src. *PLoS One* 2013; **8**(7): e71035.

114. Tigan AS, Bellutti F, Kollmann K, Tebb G, Sexl V. CDK6-a review of the past and a glimpse into the future: from cell-cycle control to transcriptional regulation. *Oncogene* 2016; **35**(24): 3083-91.

115. Eckert F, Schilbach K, Klumpp L, et al. Potential Role of CXCR4 Targeting in the Context of Radiotherapy and Immunotherapy of Cancer. *Front Immunol* 2018; **9**: 3018.

116. Johnstone CN, Pattison AD, Harrison PF, et al. FGF13 promotes metastasis of triple-negative breast cancer. *Int J Cancer* 2020; **147**(1): 230-43.

117. Nasif D, Campoy E, Laurito S, et al. Epigenetic regulation of ID4 in breast cancer: tumor suppressor or oncogene? *Clin Epigenetics* 2018; **10**(1): 111.

118. Kondo S, Iwata S, Yamada T, et al. Impact of the integrin signaling adaptor protein NEDD9 on prognosis and metastatic behavior of human lung cancer. *Clin Cancer Res* 2012; **18**(22): 6326-38.

119. Hu G, Zeng W, Xia Y. TWEAK/Fn14 signaling in tumors. *Tumour Biol* 2017; **39**(6): 1010428317714624.

120. Xiang J, Fu X, Ran W, Wang Z. Grhl2 reduces invasion and migration through inhibition of TGFbeta-induced EMT in gastric cancer. *Oncogenesis* 2017; **6**(1): e284.

121. Kou YB, Zhang SY, Zhao BL, Ding R, Liu H, Li S. Knockdown of MMP11 inhibits proliferation and invasion of gastric cancer cells. *Int J Immunopathol Pharmacol* 2013; **26**(2): 361-70.

122. Zhou H, Blevins MA, Hsu JY, et al. Identification of a Small-Molecule Inhibitor That Disrupts the SIX1/EYA2 Complex, EMT, and Metastasis. *Cancer Res* 2020; **80**(12): 2689-702.

123. Motz GT, Coukos G. The parallel lives of angiogenesis and immunosuppression: cancer and other tales. *Nat Rev Immunol* 2011; **11**(10): 702-11.

124. Gabrilovich DI, Chen HL, Cunningham HT, et al. Production of vascular endothelial growth factor by human tumors inhibits the functional maturation of dendritic cells. *Nat Med* 1996; **2**(10): 1096-103.

125. Ohm JE, Gabrilovich DI, Sempowski GD, et al. VEGF inhibits T-cell development and may contribute to tumor-induced immune suppression. *Blood* 2003; **101**(12): 4878-86.

126. Li B, Lalani AS, Harding TC, et al. Vascular endothelial growth factor blockade reduces intratumoral regulatory T cells and enhances the efficacy of a GM-CSF - Secreting cancer immunotherapy. *Clin Cancer Res* 2006; **12**(22): 6808-16.

127. Coffelt SB, Tal AO, Scholz A, et al. Angiopoietin-2 Regulates Gene Expression in TIE2-Expressing Monocytes and Augments Their Inherent Proangiogenic Functions. *Cancer Res* 2010; **70**(13): 5270-80.

128. Coffelt SB, Chen YY, Muthana M, et al. Angiopoietin 2 stimulates TIE2-expressing monocytes to suppress T cell activation and to promote regulatory T cell expansion. *J Immunol* 2011; **186**(7): 4183-90.

129. Di Tacchio M, Macas J, Weissenberger J, et al. Tumor Vessel Normalization, Immunostimulatory Reprogramming, and Improved Survival in Glioblastoma with Combined Inhibition of PD-1, Angiopoietin-2, and VEGF. *Cancer Immunol Res* 2019; **7**(12): 1910-27.

130. Fiegle E, Doleschel D, Koletnik S, et al. Dual CTLA-4 and PD-L1 Blockade Inhibits Tumor Growth and Liver Metastasis in a Highly Aggressive Orthotopic Mouse Model of Colon Cancer. *Neoplasia* 2019; **21**(9): 932-44.

131. Shapouri-Moghaddam A, Mohammadian S, Vazini H, et al. Macrophage plasticity, polarization, and function in health and disease. *J Cell Physiol* 2018; **233**(9): 6425-40.

132. Ruytinx P, Proost P, Van Damme J, Struyf S. Chemokine-Induced Macrophage Polarization in Inflammatory Conditions. *Front Immunol* 2018; **9**: 1930.

133. Park SM, Do-Thi VA, Lee JO, Lee H, Kim YS. Interleukin-9 Inhibits Lung Metastasis of Melanoma through Stimulating Anti-Tumor M1 Macrophages. *Mol Cells* 2020; **43**(5): 479-90.

134. Gao J, Zhao L, Wan YY, Zhu B. Mechanism of Action of IL-7 and Its Potential Applications and Limitations in Cancer Immunotherapy. *Int J Mol Sci* 2015; **16**(5): 10267-80.

135. Knudson KM, Hicks KC, Alter S, Schlom J, Gameiro SR. Mechanisms involved in IL-15 superagonist enhancement of anti-PD-L1 therapy. *J Immunother Cancer* 2019; **7**(1): 82.

136. Van Overmeire E, Stijlemans B, Heymann F, et al. M-CSF and GM-CSF Receptor Signaling Differentially Regulate Monocyte Maturation and Macrophage Polarization in the Tumor Microenvironment. *Cancer Res* 2016; **76**(1): 35-42.

137. Fleetwood AJ, Dinh H, Cook AD, Hertzog PJ, Hamilton JA. GM-CSF- and M-CSF-dependent macrophage phenotypes display differential dependence on type I interferon signaling. *J Leukoc Biol* 2009; **86**(2): 411-21.

138. Zhang H, Ye YL, Li MX, et al. CXCL2/MIF-CXCR2 signaling promotes the recruitment of myeloid-derived suppressor cells and is correlated with prognosis in bladder cancer. *Oncogene* 2017; **36**(15): 2095-104.

139. Scapini P, Morini M, Tecchio C, et al. CXCL1/macrophage inflammatory protein-2-induced angiogenesis in vivo is mediated by neutrophil-derived vascular endothelial growth factor-A. *J Immunol* 2004; **172**(8): 5034-40.

140. Okazaki T, Ebihara S, Takahashi H, Asada M, Kanda A, Sasaki H. Macrophage colony-stimulating factor induces vascular endothelial growth factor production in skeletal muscle and promotes tumor angiogenesis. *J Immunol* 2005; **174**(12): 7531-8.

141. Felcht M, Luck R, Schering A, et al. Angiopoietin-2 differentially regulates angiogenesis through TIE2 and integrin signaling. *J Clin Invest* 2012; **122**(6): 1991-2005.

142. Desgrosellier JS, Cheresh DA. Integrins in cancer: biological implications and therapeutic opportunities. *Nat Rev Cancer* 2010; **10**(1): 9-22.

143. Hamidi H, Ivaska J. Every step of the way: integrins in cancer progression and metastasis. *Nat Rev Cancer* 2018; **18**(9): 533-48.

144. Pedrosa AR, Bodrug N, Gomez-Escudero J, et al. Tumor Angiogenesis Is Differentially Regulated by Phosphorylation of Endothelial Cell Focal Adhesion Kinase Tyrosines-397 and -861. *Cancer Res* 2019; **79**(17): 4371-86.

145. Liu W, Kovacevic Z, Peng Z, et al. The molecular effect of metastasis suppressors on Src signaling and tumorigenesis: new therapeutic targets. *Oncotarget* 2015; **6**(34): 35522-41.

146. Kim LC, Song L, Haura EB. Src kinases as therapeutic targets for cancer. *Nat Rev Clin Oncol* 2009; **6**(10): 587-95.

147. Zhao G, Gong L, Su D, et al. Cullin5 deficiency promotes small-cell lung cancer metastasis by stabilizing integrin beta1. *J Clin Invest* 2019; **129**(3): 972-87.

148. Aboubakar Nana F, Hoton D, Ambroise J, et al. Increased Expression and Activation of FAK in Small-Cell Lung Cancer Compared to Non-Small-Cell Lung Cancer. *Cancers (Basel)* 2019; **11**(10).

149. Serrels A, Lund T, Serrels B, et al. Nuclear FAK Controls Chemokine Transcription, Tregs, and Evasion of Anti-tumor Immunity. *Cell* 2015; **163**(1): 160-73.

150. Jiang H, Hegde S, Knolhoff BL, et al. Targeting focal adhesion kinase renders pancreatic cancers responsive to checkpoint immunotherapy. *Nat Med* 2016; **22**(8): 851-+.

151. Dong Z, Chen J, Yang X, et al. Ang-2 promotes lung cancer metastasis by increasing epithelial-mesenchymal transition. *Oncotarget* 2018; **9**(16): 12705-17.

152. Chen MB, Lamar JM, Li R, Hynes RO, Kamm RD. Elucidation of the Roles of Tumor Integrin beta1 in the Extravasation Stage of the Metastasis Cascade. *Cancer Res* 2016; **76**(9): 2513-24.

153. Oshita F, Kameda Y, Hamanaka N, et al. High expression of integrin beta1 and p53 is a greater poor prognostic factor than clinical stage in small-cell lung cancer. *Am J Clin Oncol* 2004; **27**(3): 215-9.

154. Lawson MH, Cummings NM, Rassl DM, et al. Bcl-2 and beta1-integrin predict survival in a tissue microarray of small cell lung cancer. *Br J Cancer* 2010; **103**(11): 1710-5.

155. Ebos JM, Kerbel RS. Antiangiogenic therapy: impact on invasion, disease progression, and metastasis. *Nat Rev Clin Oncol* 2011; **8**(4): 210-21.

156. Kuczynski EA, Vermeulen PB, Pezzella F, Kerbel RS, Reynolds AR. Vessel co-option in cancer. *Nat Rev Clin Oncol* 2019; **16**(8): 469-93.

157. Li P, Sun T, Yuan Q, Pan G, Zhang J, Sun D. The expressions of NEDD9 and E-cadherin correlate with metastasis and poor prognosis in triple-negative breast cancer patients. *Onco Targets Ther* 2016; **9**: 5751-9.

158. Jin Y, Li F, Zheng C, et al. NEDD9 promotes lung cancer metastasis through epithelial-mesenchymal transition. *Int J Cancer* 2014; **134**(10): 2294-304.

159. Sima N, Cheng X, Ye F, Ma D, Xie X, Lu W. The overexpression of scaffolding protein NEDD9 promotes migration and invasion in cervical cancer via tyrosine phosphorylated FAK and SRC. *PLoS One* 2013; **8**(9): e74594.

160. Liu T, Yu J, Deng M, et al. CDK4/6-dependent activation of DUB3 regulates cancer metastasis through SNAIL1. *Nat Commun* 2017; **8**: 13923.

161. Goel S, Bergholz JS, Zhao JJ. Targeting CDK4 and CDK6 in cancer. *Nat Rev Cancer* 2022; **22**(6): 356-72.

7 LIST OF FIGURES

8 VORABVERÖFFENTLICHUNG VON ERGEBNISSEN

Diese Arbeit ist teilweise in Anlehnung und Zusammenarbeit mit der noch unveröffentlichten Publikation mit dem vorläufigen Titel „*Blocking the Angiopoietin-2/integrin beta-1 signaling axis abrogates tumor cell invasion and metastasis in small cell lung cancer*" von Meder *et al.* (Ersteinreichung am 18.10.2022 bei „*JCI Insight",* Manuskript 166402-INS-RG-1) entstanden. Weitere in der Publikation gelistete Mitautoren waren an der Entstehung dieser Arbeit über diesen Weg mittelbar beteiligt. In dieser Arbeit werden Inhalte, die aus der noch unveröffentlichten Publikation Meder *et al.* mit freundlicher Genehmigung übernommen wurden, entsprechend zitiert und als *„under revision"* gekennzeichnet. Das schriftliche Einverständnis von Univ.-Prof. Dr. Dr. Roland Ullrich über die Vorabveröffentlichung von Teilergebnissen in dieser Arbeit liegt vor.